CHAPTER IV

RESULTS AND DISCUSSION

4.1. Influence of silica precursors and mole ratios of CTAB/silica precursor on the synthesis and properties of non-doped and HPMSP doped mesoporous silica

4.1.1. Synthesis of materials

In combining three types of silica precursor with three mole ratios of CTAB/silica precursor, nine types of non-doped and HPMSP doped mesoporous silica were prepared as shown in Table 4.1.

Table 4.1 Types of non-doped and HPMSP doped mesoporous silica prepared from different types of silica precursors and various mole ratios of CTAB/silica precursor.

Type of silica precursor	CTAB/silica precursor (mole ratio)	Name of mesoporous silica	
		Non-doped	HPMSP-doped
TEOS	0	TA	TDA
	0.09	TB	TDB
	0.18	TC	TDC
Calcined mesoporous silica	0	MA	MDA
	0.09	MB	MDB
	0.18	MC	MDC
Silica gel 60	0	SA	SDA
	0.09	SB	SDB
	0.18	SC	SDC

From the synthesis results, it was found that all types of mesoporous silica could be successfully prepared except TA and TDA for which TEOS was used as a silica precursor and the mole ratio of CTAB/silica precursor equaled to 0. For the achieved synthesis, after 5 minutes of the addition of silica precursor, the fluid mixture became progressively turbid due to the appearance of silica. During the filtration process, the difficulty in the separation of silica was found for TB, TDB, SA and SDA. These materials were then separated by centrifugation. On the contrary, the filtration was so facile for other mesoporous silica.

The determination of HPMSP molecules in the supernatant and washing solutions of all successful syntheses by UV-Vis spectrophotometer revealed the

inexistence of HPMSP molecules in all solutions. Accordingly, it could be concluded that all doping molecules were achieve incorporated in each type of HPMSP doped mesoporous silica.

4.1.2. Characterization of materials

The characterization of materials was performed for the achieved synthesized non-doped and HPMSP doped mesoporous silica. The details of each result were written as follow.

4.1.2.1. Determination of organic matters in silica

The organic matters in non-doped and HPMSP doped mesoporous silica determined by calcination (namely measured value) and those calculated from starting materials (namely calculated value) as described in Appendix IV were tabulated in Tables 4.2 and 4.3.

Table 4.2 Amounts of organic matters in non-doped mesoporous silica.

Silica precursor	CTAB / Silica precursor (mole ratio)	Organic matters (%)		measured value / calculated value x 100 (%)
		measured value	calculated value	
TEOS	0.09	41.72	29.89	139.6
	0.18	53.27	46.02	115.8
Calcined mesoporous silica	0	10.08	0	-
	0.09	34.83	29.64	117.5
	0.18	41.96	46.06	91.09
Silica gel 60	0	11.30	0	-
	0.09	32.46	29.64	109.5
	0.18	46.41	46.06	100.8

ศูนย์วิทยทรัพยากร
จุฬาลงกรณ์มหาวิทยาลัย

Table 4.3 Amounts of organic matters in HPMSP doped mesoporous silica.

Silica precursor	CTAB / Silica precursor (mole ratio)	Organic matters (%)		measured value / calculated value x 100 (%)
		measured value	calculated value	
TEOS	0.09	45.27	46.40	97.56
	0.18	58.75	56.36	104.2
Calcined mesoporous silica	0	25.78	30.53	84.44
	0.09	49.85	46.26	107.8
	0.18	59.02	56.39	104.7
Silica gel 60	0	27.58	30.53	90.34
	0.09	52.37	46.25	113.2
	0.18	54.26	56.39	96.22

As shown in Tables 4.2 and 4.3, the organic matter contents obtained from the experiment were close to the values calculated from the starting materials. These results mean that not only the doping molecules but also that of surfactant are well incorporated in silica. For some experimental results which were slightly higher than the theoretical values, it may be explained by the amounts of physisorbed water and chemisorbed water remained in the silica framework before the beginning of calcination process. Actually, the removal of physisorbed water and chemisorbed water is achieved at 170 °C and 400 °C, respectively [14]. On the contrary, for the experimental results which were slightly lower than the calculated values, these minor differences were probably due to the loss of some surfactant. Actually, the latter was observed in the form of bubbles during the washing step. To measure the fraction weight lost during the calcination process, the thermogravimetric analysis–mass spectrometer (TGA-MS) ought to be used.

4.1.2.2. Investigation of organic molecules in mesoporous silica by FTIR spectroscopy

The presence of organic matters including HPMSP and CTAB molecules in the modified materials could be determined using FT-IR technique. The resulting spectras of non-doped and HPMSP-doped mesoporous silica were exhibited in Figures 4.1 and 4.2, respectively.

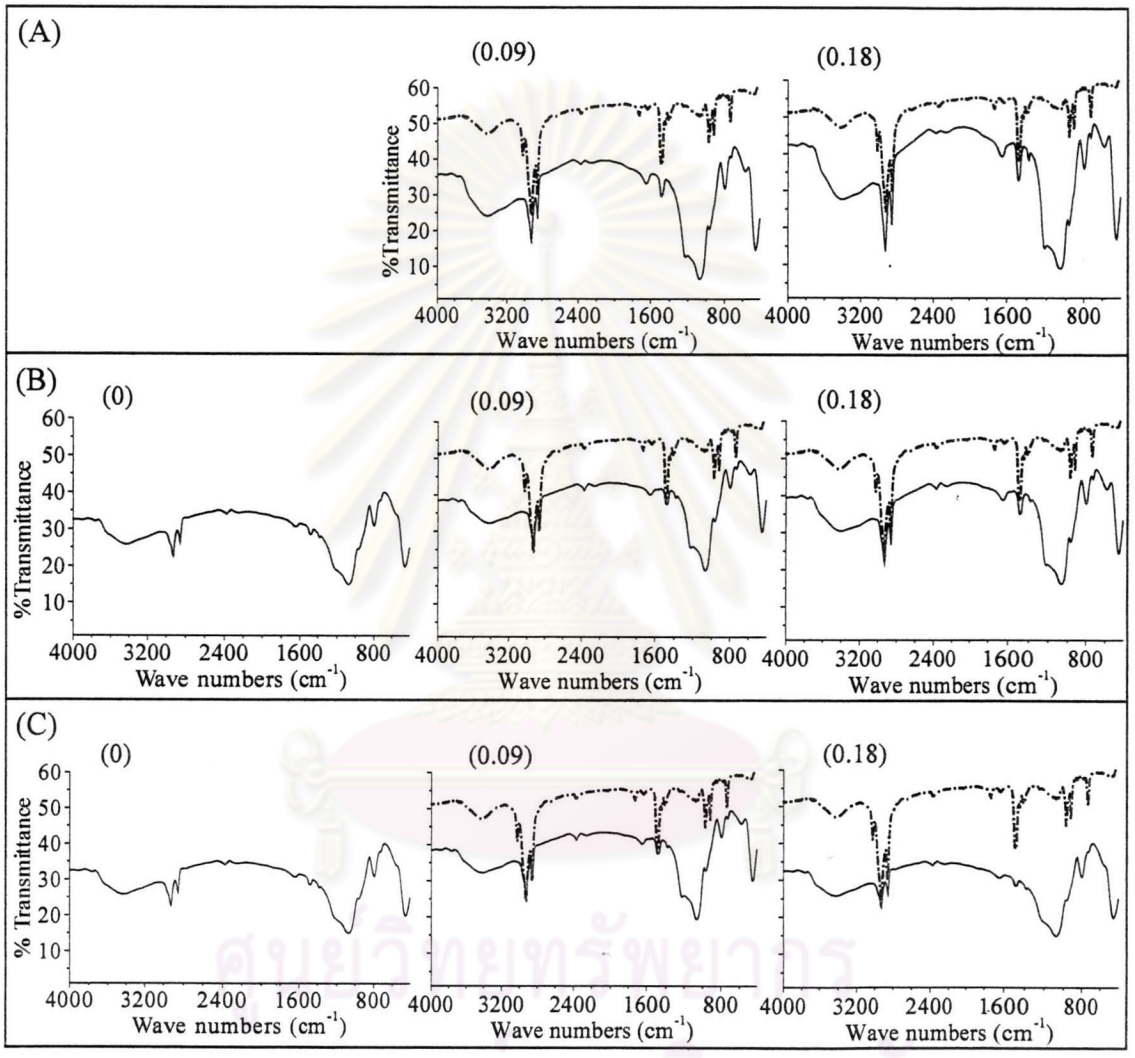

Figure 4.1 FT-IR spectra of non-doped mesoporous silica synthesized from various precursor: (A) TEOS, (B) calcined mesoporous silica and (C) silica gel 60. The numbers in the bracket refer to the mole ratio of CTAB/silica precursor (dash-dot: CTAB, solid: non-doped mesoporous silica)

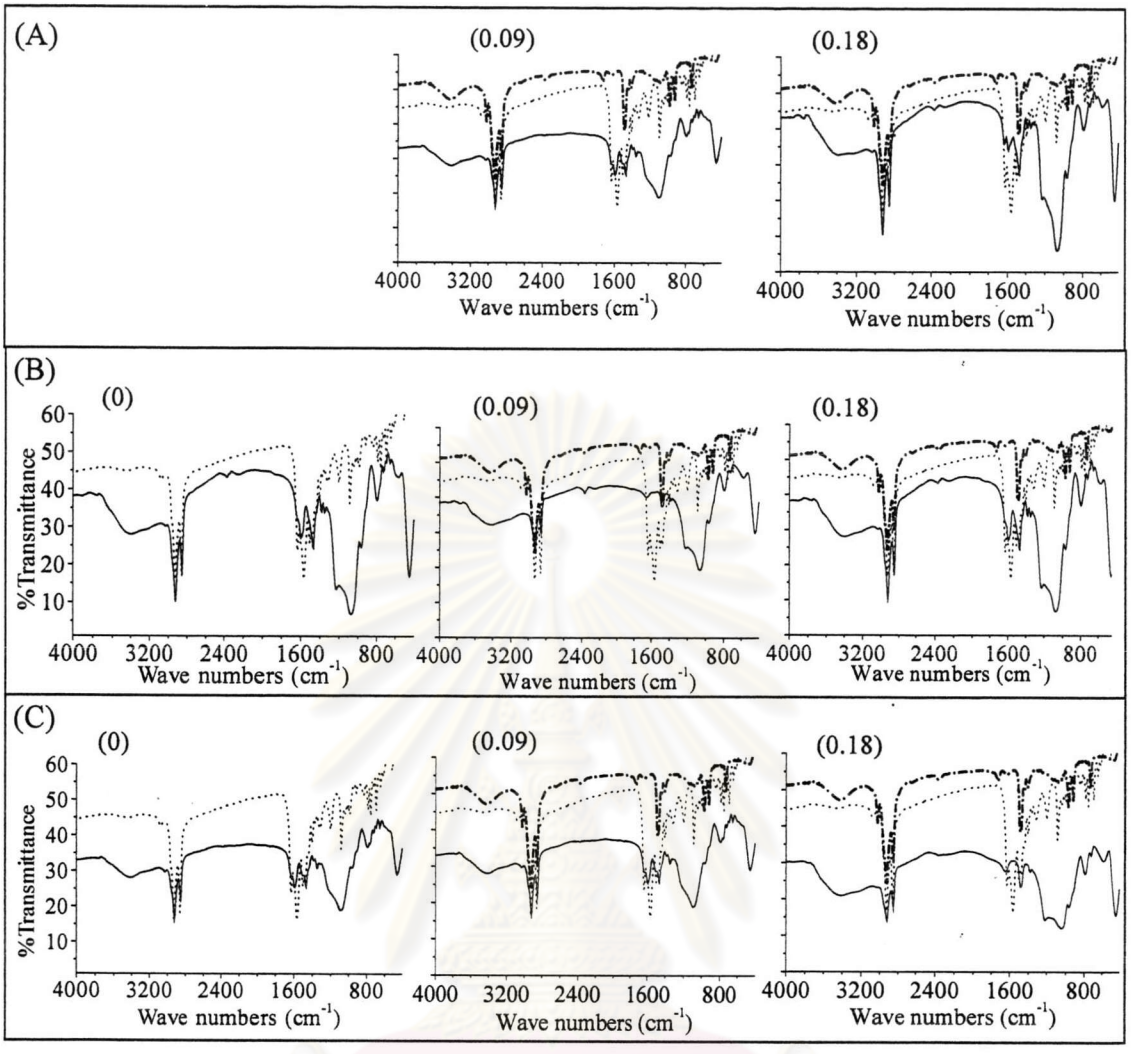

Figure 4.2 FT-IR spectra of HPMSP doped mesoporous silica synthesized from various precursors: (A) TEOS, (B) calcined mesoporous silica and (C) silica gel 60. The numbers in the bracket refer to the mole ratio of CTAB/silica precursor (dash-dot: CTAB, dot: HPMSP, solid: HPMSP doped mesoporous silica)

As shown in Figure 4.1, the FT-IR spectra of all non-doped mesoporous silica showed the characteristic bands of silica [14]. The peak at about 3416 cm^{-1} was assigned to the hydrogen-bonded SiOH groups perturbed by physically adsorbed water. The bands of the silica framework were also shown at 1050 cm^{-1} and 794 cm^{-1}, corresponded to the vibration of the asymmetric and symmetric stretching of Si-O modes, respectively. The band of Si-O-Si bending mode appeared at 456 cm^{-1}. In addition, the characteristic bands of CTAB at 2925, 2848 and 1482 cm^{-1} attributed to CH stretching were also observed in all spectra of non-doped mesoporous silica. These results suggested that the templated molecules were actually contained in these sorbents.

The characteristic bands of silica and CTAB were also observed in all FT-IR spectra of HPMSP doped mesoporous silica. Furthermore, two characteristic bands corresponded to C=O stretching and aromatic C=C stretching of the pyrazolone group were also shown at 1634 and 1588 cm^{-1}, respectively. These FT-IR results were the evidence of the presence of HPMSP molecules in the modified silica.

4.1.2.3. Determination of accessible HPMSP

The determination of accessible HPMSP is aimed at investigating the active HPMSP molecules in the modified mesoporous silica. The experimental procedure followed the method described by Boos *et al.* [29]. 10 mL of the mixture of heptane and EtOH with the volume ratio of 1 : 1 were used as an extracting solvent. The obtained results had shown that all incorporated HPMSP molecules could be completely extracted from silica. So it could be concluded that the accessibility of these molecules to the extracting solvent is excellent. This observation is in accordance with the results reported in previous works [29, 39].

4.1.2.4. Crystallinity of materials

X-ray diffraction is a typical technique for the investigation of structure and crystallinity of materials. The diffractrograms of all as-synthesized materials and the corresponding calcined silica were presented in Figures 4.3 and 4.4, respectively. As seen, the crystal structure of the as-synthesized materials was obtained when the silica precursor was TEOS or calcined mesoporous silica. However, the mole ratio of CTAB/silica precursor should be greater than or equal to 0.09. On the contrary, the structure of all as-synthesized silicas prepared from silica gel 60 was amorphous. These results implied that not only the silica precursor but also the mole ratio of CTAB/silica precursor played a crucial role for the structure of such materials.

Considering the XRD patterns of most calcined materials, the diffraction peaks disappeared indicating a significant degradation of the solid. For the XRD pattern of the calcined non-doped mesoporous silica synthesized from 0.18 CTAB/TEOS mole ratio, the intensity of this spectra was found to be higher than that of the corresponding as-synthesized sorbent. This observation indicated the better-defined structure of materials and a slight shrinkage in pore size due to the condensation of SiOH group after calcination.

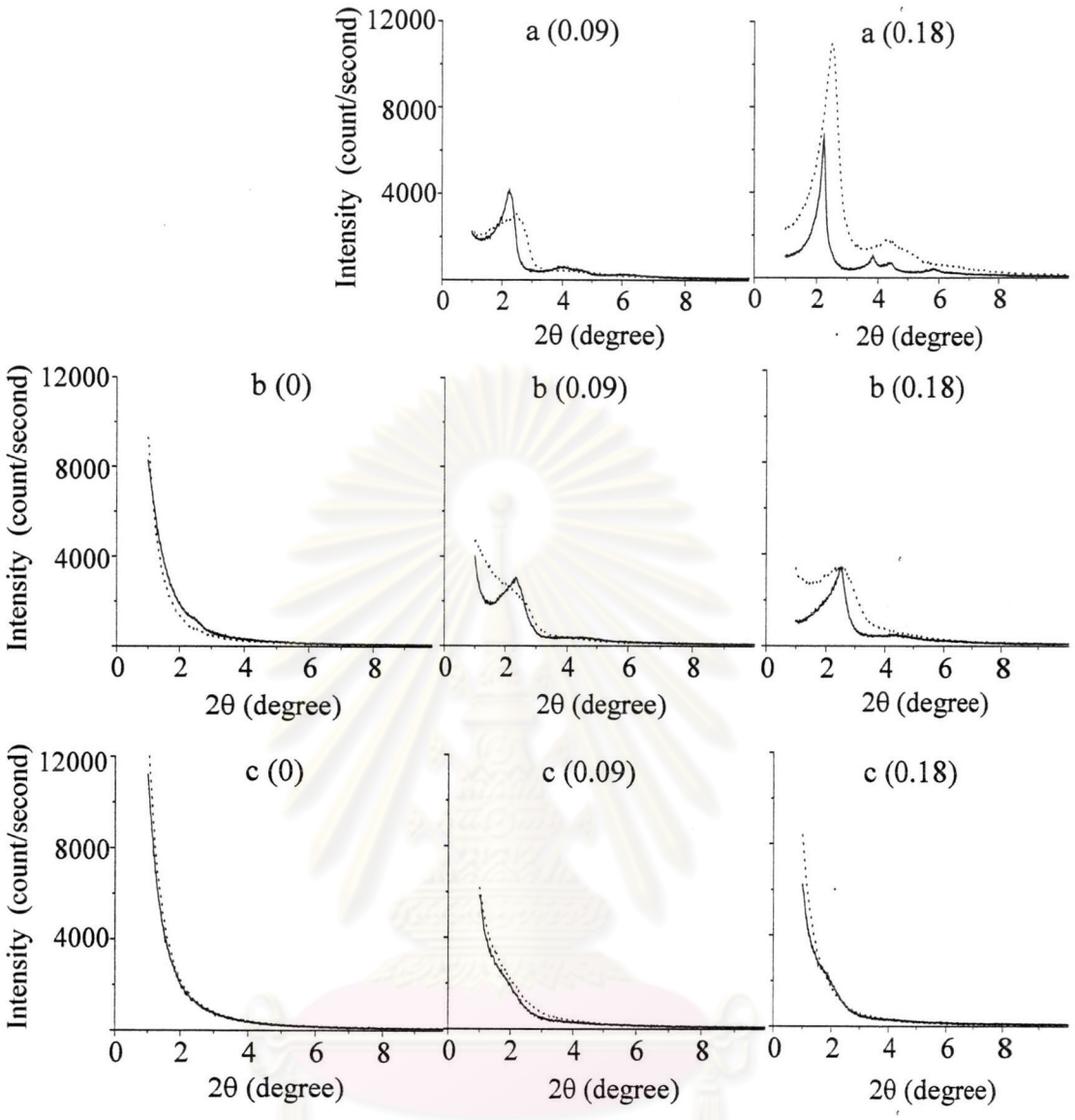

Figure 4.3 XRD patterns of non-doped mesoporous silica synthesized from various precursors: (a) TEOS, (b) calcined mesoporous silica and (c) silica gel 60. The numbers in the parenthesis referred to the mole ratio of CTAB/silica precursor used for the synthesis (solid line: as synthesized silica, dot line: calcined silica).

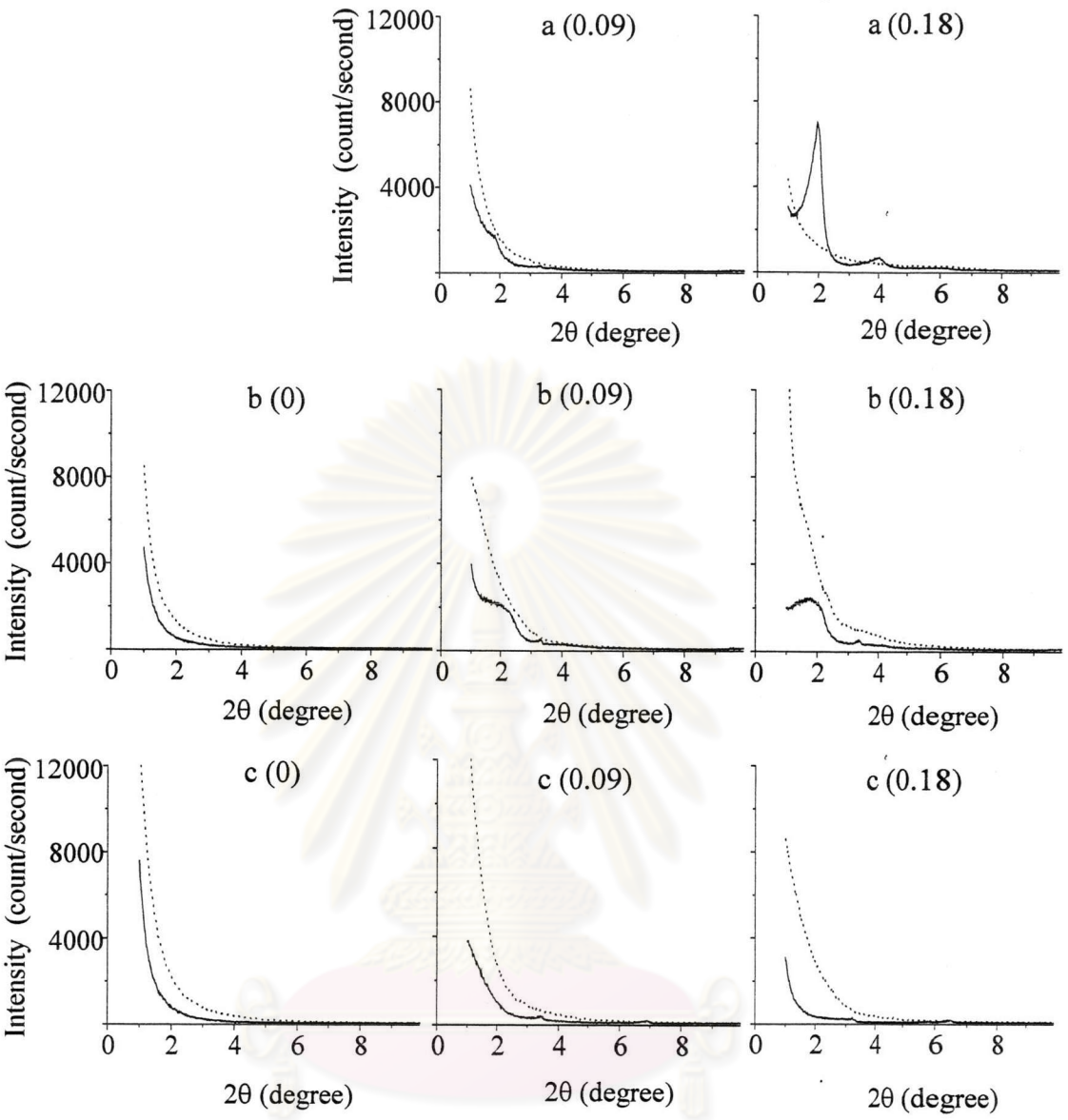

Figure 4.4 XRD patterns of HPMSP doped mesoporous silica synthesized from various precursors: (a) TEOS, (b) calcined mesoporous silica and (c) silica gel 60. The numbers in the parenthesis referred to the mole ratio of CTAB/silica precursor used for the synthesis (solid line: as synthesized silica, dot line: calcined silica).

Tables 4.4 and 4.5 showed the d-spacing values of non-doped and HPMSP doped mesoporous silica, respectively. As seen, these values decreased considerably after calcination. The explanation of these results may be attributed to the condensation of the silanol groups in the channel walls concomitant with the removal of the surfactant template from the channels.

Table 4.4 XRD results of non-doped mesoporous silica synthesized from various silica precursors and different CTAB/silica precursor mole ratios.

Silica precursor	mole ratio of CTAB : silica precursor	As-synthesized silica		Calcined silica	
		2θ (degree)	d-spacing (Å)	2θ (degree)	d-spacing (Å)
TEOS	0.09	2.260 4.060 4.659	39.06 21.74 18.95	2.500	35.31
	0.18	2.238 3.840 4.381 5.859	39.44 22.99 20.15 15.07	2.500 4.440 4.969	35.31 19.88 17.77
Calcined mesoporous silica	0	-	-	-	-
	0.09	2.360	37.40	2.250 2.650	39.23 33.32
	0.18	2.520 4.436	35.03 19.90	2.580	34.22
Silica gel 60	0	-	-	-	-
	0.09	1.870	47.21	2.129	41.46
	0.18	1.750	50.45	-	-

Table 4.5 XRD results of HPMSP doped mesoporous silica synthesized from various silica precursors and different CTAB/silica precursor mole ratios.

Silica precursor	mole ratio of CTAB : silica precursor	As-synthesized silica		Calcined silica	
		2θ (degree)	d-spacing (Å)	2θ (degree)	d-spacing (Å)
TEOS	0.09	1.789	49.33	-	-
	0.18	1.960 4.039	45.03 21.86	1.309	67.42
Calcined mesoporous silica	0	2.510	35.17	-	-
	0.09	2.290	38.55	-	-
	0.18	2.319	38.06	-	-
Silica gel 60	0	-	-	-	-
	0.09	3.420 6.918	25.82 12.77	2.840	31.08
	0.18	1.940 3.341	45.51 26.42	1.649 2.369 4.018	53.52 37.26 21.97

4.1.2.5. Surface area, pore volume and pore size

Nitrogen sorption analysis is a well-known method for determination of surface area and textural properties of materials. This technique was then applied to characterize the morphology of sorbents in this work. The specific surface area of the functionalized materials was determined through the BET method. The pore size distribution of the sorbents was analyzed according to the BJH model. The pore volume of the calcined silica was calculated from the desorption volume at P/P_0 equal to 0.99.

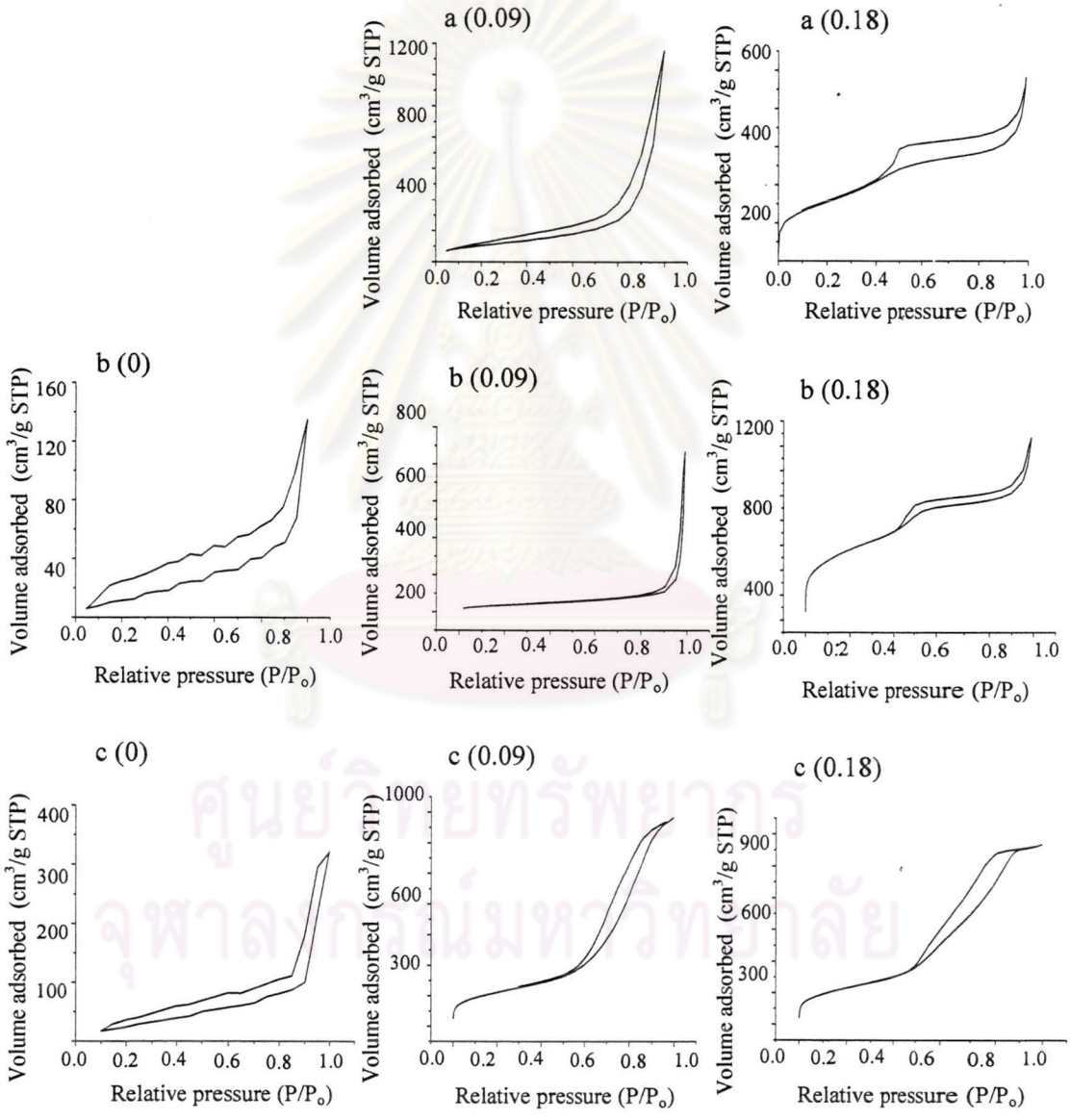

Figure 4.5 Nitrogen sorption isotherms of HPMSP doped mesoporous silica synthesized from various precursors: (a) TEOS, (b) calcined mesoporous silica, (c) silica gel 60. The numbers in the parenthesis referred to the mole ratio of CTAB/silica precursor used for the synthesis.

The nitrogen sorption isotherms of different HPMSP modified sorbents were shown in Figure 4.5. According to IUPAC, all isotherms could be classified as a type IV isotherm with a H3 or H4 hysteresis loop characteristic of mesoporous material with aggregates of plate-like particles and slit-shaped pores. Figure 4.6 showed the pore size distribution of various HPMSP mesoporous silica. The narrow pore size distribution was observed when the material was synthesized with the CTAB/silica precursor mole ratio of 0.09 or greater.

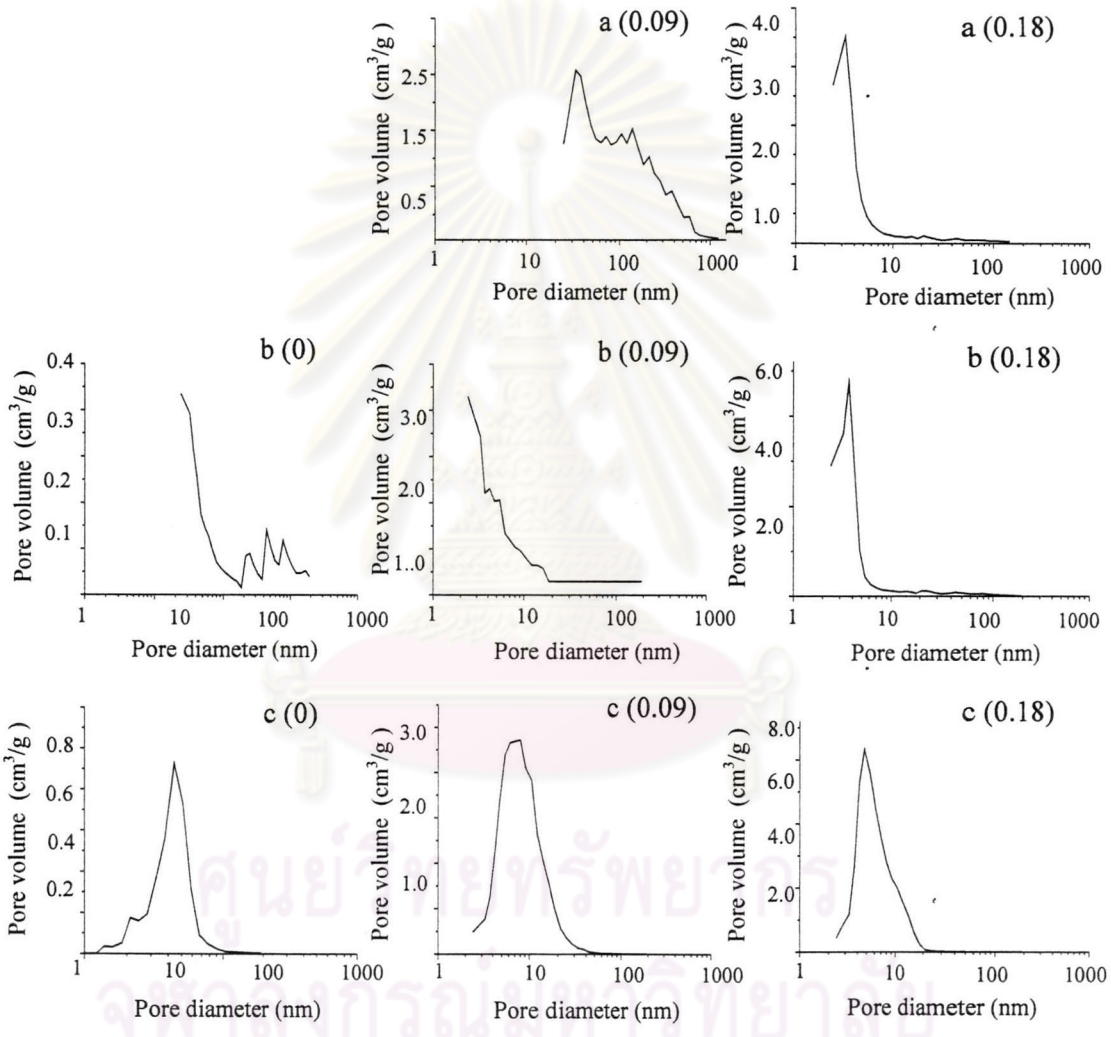

Figure 4.6 BJH pore diameters of HPMSP doped mesoporous silica synthesized from various precursors: (a) TEOS, (b) calcined mesoporous silica, (c) silica gel 60. The numbers in the parenthesis referred to the mole ratio of CTAB/silica precursor used for the synthesis.

Table 4.6 displayed the BET surface area, pore volume and average pore diameter of different HPMSP doped mesoporous silica. Their surface area seemed to be increased with the increasing of CTAB contents. These results meant that the

increase in template concentration promoted the ordered structural formation of materials.

Table 4.6 Characterization results of different calcined HPMSP-doped mesoporous silicas determined from N_2 sorption experiment at 77 K and XRD measurement.

Type of silica		S (m^2/g)	Vp (cm^3/g)	APD (nm)	d_{100} (nm)	a_0 (nm)	w (nm)
Silica precursor	CTAB / Silica precursor (mole ratio)						
TEOS	0.09	392	1.52	15.51	-	-	-
	0.18	550	0.74	5.38	6.74	23.34	17.96
Calcined mesoporous silica	0	20	0.13	26.00	-	-	-
	0.09	34	0.33	38.82	-	-	-
	0.18	503	0.57	4.53	-	-	-
Silica gel 60	0	142	1.21	34.08	-	-	-
	0.09	397	1.05	10.58	3.11	10.77	0.19
	0.18	410	0.88	8.59	3.73	12.92	4.33

S, BET surface area (m^2/g) obtained from N_2 sorption; V_p, Total pore volume (cm^3/g) obtained from single-point volume at $P/P_o = 0.99$; *APD*, average pore diameter calculated from $4Vp/S$; d_{100}, d-value 100 reflections; a_o = the lattice parameter, from the XRD data using the formula $a_o = 2d_{100}\sqrt{3}$; *w*, pore wall thickness was equaled to a_o-*APD*.

For the non-doped mesoporous silica, only the materials which were synthesized from TEOS were used as a comparative sorbent. Their N_2 sorption isotherms shown in Figure 4.7 exhibited similar type as observed for the HPMSP modified sorbent. The BJH results illustrated in Figure 4.8 confirmed the mesopore of material with narrow pore size distribution. The summary of the textural morphologies of non-doped material were listed in Table 4.7.

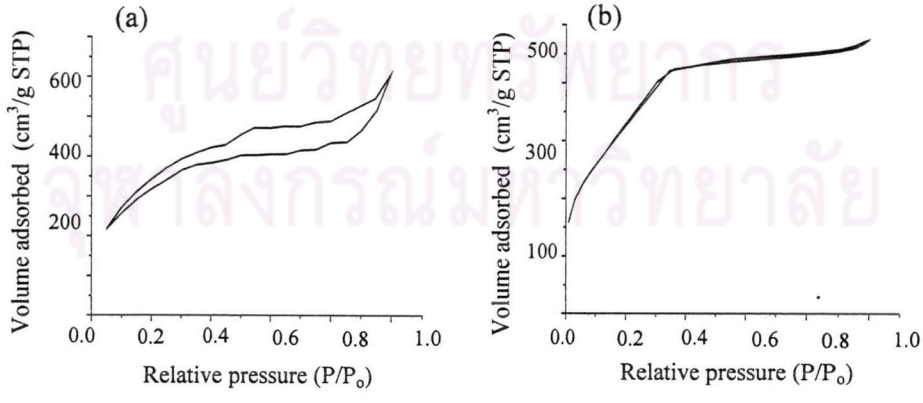

Figure 4.7 Nitrogen sorption isotherms of non-doped mesoporous silica synthesized from TEOS with different mole ratios of CTAB/TEOS: (a) 0.09 and (b) 0.18.

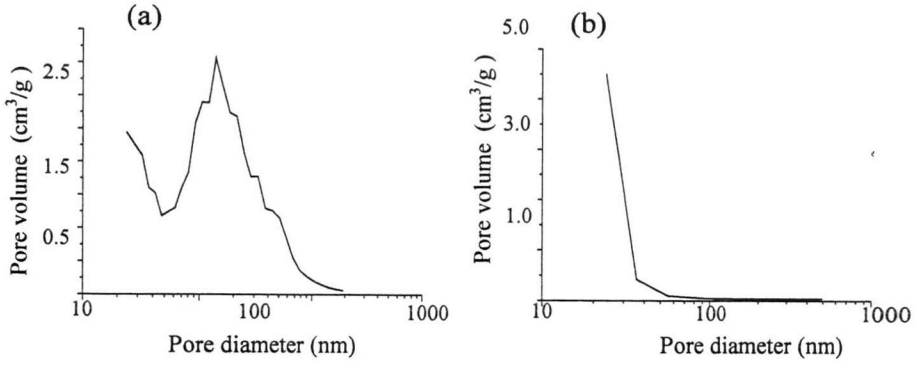

Figure 4.8 BJH pore diameters of non-doped mesoporous silica synthesized from TEOS with different mole ratios of CTAB/TEOS: (a) 0.09 and (b) 0.18.

Table 4.7 Characterization results of calcined non-doped mesoporous silica synthesized from TEOS determined from N_2 sorption experiment at 77 K and XRD measurement.

CTAB/TEOS (mole ratio)	S (m^2/g)	Vp (cm^3/g)	APD (nm)	d_{100} (nm)	a_0 (nm)	w (nm)
0.09	1158	0.94	3.24	3.53	12.23	8.99
0.18	1059	0.72	2.72	3.53	12.23	9.51

S, BET surface area (m^2/g) obtained from N_2 sorption; V_p, Total pore volume (cm^3/g) obtained from single-point volume at $P/P_o = 0.99$; *APD*, average pore diameter calculated from $4Vp/S$; d_{100}, d-value 100 reflections; a_o = the lattice parameter, from the XRD data using the formula $a_o = 2d_{100}\sqrt{3}$; *w*, pore wall thickness was equaled to a_o-*APD*.

Considering the surface area of both sorbents synthesized from TEOS, it was found that the surface area of the HPMSP modified sorbent was lower than that of the corresponding non-doped mesoporous silica. The decrease in surface area after the incorporation of the doping molecules might be due to the presence of pendant groups which partially blocked the adsorption of nitrogen molecules on the surface and consequently caused a decrease in the surface area. In addition, the pore volume and the average pore diameter of the HPMSP doped mesoporous silica seem to be higher than that of non-doped materials. These phenomena could be explained by the incorporated HPMSP which provided an expansion of the pore size and a decrease in the void fraction. Furthermore, the pore wall thickness of silica was observed.

4.1.2.6. Morphology of materials

The morphology of both as-synthesized non-doped and HPMSP doped mesoporous silica synthesized from various silica precursors with the mole ratio of CTAB/silica precursor equal to 0.18 was examined using scanning electron microscopy (SEM) technique. The SEM images results of non-doped and HPMSP doped mesoporous silica were displayed in Figures 4.9 and 4.10, respectively.

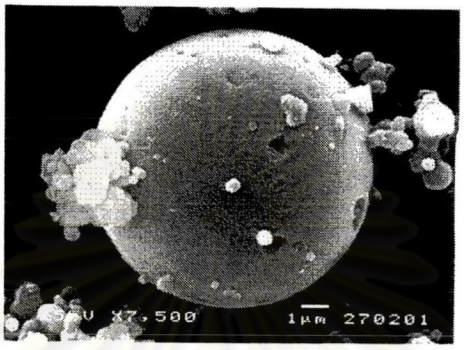

Figure 4.9 SEM image of non-doped mesoporous silica prepared with TEOS as a silica precursor.

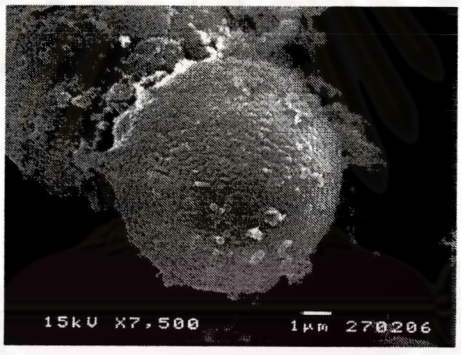

(a)

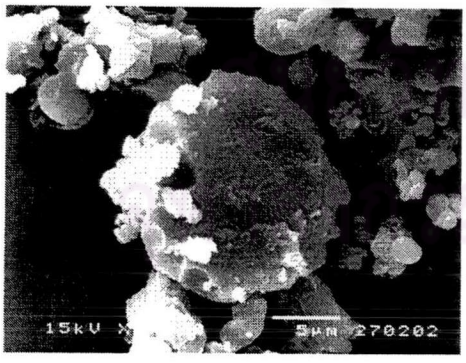

(b)

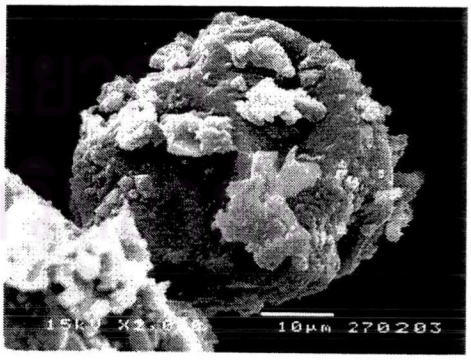

(c)

Figure 4.10 SEM images of HPMSP doped mesoporous silica synthesized from silica precursor: (a) TEOS, (b) calcined mesoporous silica and (c) silica gel 60.

The SEM image of non-doped mesoporous silica revealed the round particle of this material with some aggregates of smaller particles. The particle of HPMSP

doped mesoporous silica synthesized from TEOS was also spherical and its surface looked like orange peel. Indeed, Boos and coworkers reported the multilamellar vesicles of the surface of this modified sorbent [29]. For the HPMSP modified materials synthesized from the calcined mesoporous silica or the silica gel 60, their morphologies appeared lesser spheroid with much more aggregates. However, the particle sizes of all synthesized sorbents were in the range of 10 to 45 μm.

4.1.3. Extraction properties of materials

From previous researches [29, 39], the HPMSP doped mesoporous silica was reported as an excellent sorbent for the extraction of Cu(II) ions especially when the extraction medium was 0.1 M $NaNO_3$ solution at pH 2. This condition was thus applied in this work to investigate the Cu(II) extractability of various HPMSP doped mesoporous silica. The experiment was repeated three times and the results were plotted between the amounts of Cu(II) extracted and the type of silica precursor as shown in Figure 4.11.

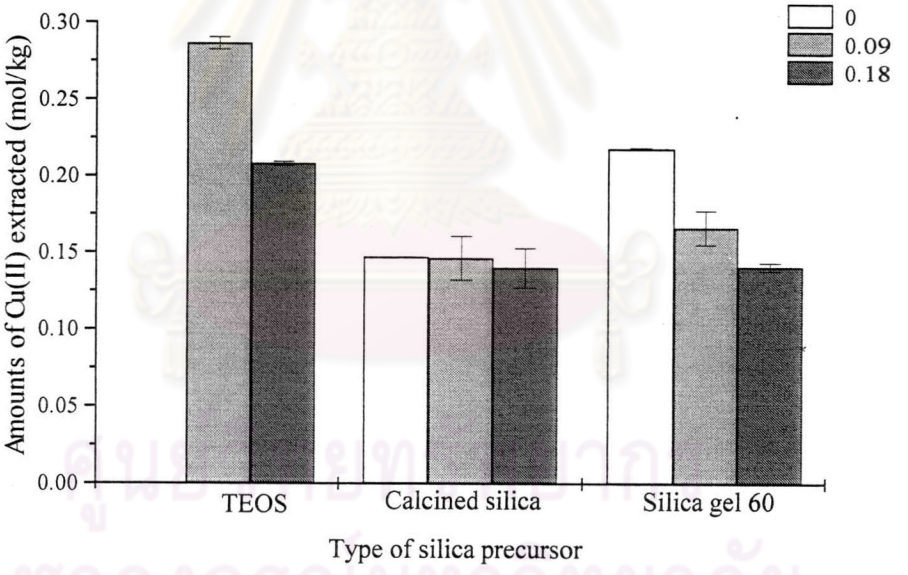

Figure 4.11 The Cu(II) extractability of HPMSP doped mesoporous silica synthesized from various silica precursors and different mole ratios of CTAB/Silica precursor.

From Figure 4.11, it could obviously be seen that all types of the HPMSP modified silica could extract the Cu(II) ions quantitatively. Indeed, after placing the functionalized sorbents in contact with the Cu(II) solution the color of these materials was immediately changed to green which was the characteristic of a $Cu(PMSP)_2$ complex. Considering the effect of various mole ratios of CTAB/silica precursor on the extraction properties of such materials, it was found that the Cu(II) extractability

of the silica was decreased with the increasing of the CTAB/silica precursor mole ratio when the silica precursor was TEOS or silica gel 60. On the contrary, these mole ratios did not have any influence on the Cu(II) extractability of the silica synthesized from calcined material. However, the reason for these phenomena is still not clear to us.

In addition, among various sorbents studied, the silica synthesized from TEOS and especially with the mole ratio of CTAB/TEOS equal to 0.09 had shown the highest Cu(II) extractability. Consequently, further experiments were focused on the use of TEOS as a silica precursor for the profound study of the synthesis of materials and their extraction properties.

4.2. Influence of CTAB/TEOS mole ratios on the synthesis and properties of non-doped and HPMSP doped mesoporous silica

4.2.1. Synthesis of materials

The results from previous section revealed that the mole ratio of CTAB/TEOS used for the synthesis of mesoporous silica played an important role for the properties of synthesized materials, especially for the Cu(II) extractability of HPMSP doped mesoporous silica. Thus, in this section, profound study was focused on the effect of CTAB/TEOS mole ratio on the synthesis and properties of materials. Five mole ratios of CTAB/TEOS such as 0.09, 0.12, 0.18, 0.24 and 0.30 were used for the synthesis of non-doped and HPMSP doped mesoporous silica. The synthesis results had shown that both non-doped and HPMSP doped mesoporous silica could be successfully synthesized. All obtained materials, except the one which was synthesized from the mole ratio CTAB/TEOS equal to 0.09, could be filtered easily. Furthermore, the results from UV spectroscopy revealed that all HPMSP molecules used in the synthesis could be successfully incorporated into all types of HPMSP doped mesoporous silica.

4.2.2. Characterization of materials

4.2.2.1. Determination of organic matters

The organic matter contents in non-doped and HPMSP doped mesoporous silica synthesized from different mole ratios of CTAB/TEOS were shown in Table 4.8 and Table 4.9, respectively. It was found that their measured values were close to the calculated values. These results implied that all the organic molecules were successfully incorporated inside the silica.

Table 4.8 The organic matter contents in non-doped mesoporous silica synthesized from different mole ratios of CTAB/TEOS.

CTAB/TEOS (mole ratio)	Organic matters (%)		$\frac{\text{measured value}}{\text{calculated value}} \times 100$ (%)
	measured value	calculated value	
0.09	33.17	29.89	110.9
0.12	39.53	36.24	109.1
0.18	49.26	46.02	107.0
0.24	54.93	53.20	103.2
0.30	53.79	58.69	91.65

Table 4.9 The organic matter contents in HPMSP doped mesoporous silica synthesized from different mole ratios of CTAB/TEOS.

CTAB/TEOS (mole ratio)	Organic matters (%)		$\frac{\text{measured value}}{\text{calculated value}} \times 100$ (%)
	measured value	calculated value	
0.09	45.27	46.40	97.56
0.12	55.03	50.21	109.6
0.18	58.75	56.36	104.2
0.24	62.98	61.18	102.9
0.30	64.72	65.04	99.51

4.2.2.2. Elemental analysis

The organic matters in mesoporous silica could also be determined using elemental analysis. This technique provided the data on the basis of C, H, N measurements. The elemental mass of both non-doped and HPMSP-doped mesoporous silica from three replicated experiments and those calculated from the composition of starting materials (shown in Appendix V) were collected in Tables 4.10 and 4.11 below.

Table 4.10 Elemental analysis results of non-doped mesoporous silica synthesized by the mole ratio of CTAB/TEOS equaled to 0.18.

CTAB/TEOS (mole ratio)	% C		% H		% N	
	experiment	theory	experiment	theory	experiment	Theory
0.18	34.42 ± 0.11	36.91	7.60 ± 0.10	6.85	2.07 ± 0.09	2.27

Table 4.11 Elemental analysis results of different HPMSP-doped mesoporous silica synthesized from various mole ratios of CTAB/TEOS.

CTAB/TEOS (mole ratio)	% C		% H		% N	
	experiment	theory	experiment	theory	experiment	theory
0.09	40.47 ± 0.06	36.33	6.56 ± 0.24	5.77	3.03 ± 0.19	2.62
0.12	42.49 ± 0.18	39.44	7.76 ± 0.18	6.42	2.82 ± 0.12	2.79
0.18	44.18 ± 0.08	44.48	7.87 ± 0.05	7.46	2.89 ± 0.26	3.05
0.24	45.38 ± 0.08	48.43	8.99 ± 0.18	8.28	3.03 ± 0.04	3.26
0.30	46.03 ± 0.06	51.58	9.47 ± 0.06	8.94	3.13 ± 0.23	3.42

From Tables 4.10 and 4.11, the experimental values of organic matter contents in all materials studied were higher than those of theoretical values of such sorbents. Therefore, these elemental analysis results confirmed the existence of CTAB and/or HPMSP molecules in the related mesoporous silica.

4.2.2.3. Investigation of organic molecules in mesoporous silica synthesized from various mole ratios of CTAB/TEOS by FTIR spectroscopy

The FT-IR spectra of non-doped and HPMSP doped mesoporous silica synthesized with difference mole ratios of CTAB/TEOS were depicted in Figures 4.12 and 4.13, respectively. From those figures, the characteristic bands of silica, CTAB and HPMSP were still observed in all FT-IR spectra of both materials synthesized with difference mole ratios of CTAB/TEOS. These results confirmed the existence of incorporated organic molecules in the related mesoporous silica. However, the difference in the amounts of CTAB contained in the silica could not be determined from these spectra since the characteristic bands of CTAB appeared at the same position as those of HPMSP. In addition, the FT-IR spectrometry was not considered as a technique for quantitative analysis.

ศูนย์วิทยทรัพยากร
จุฬาลงกรณ์มหาวิทยาลัย

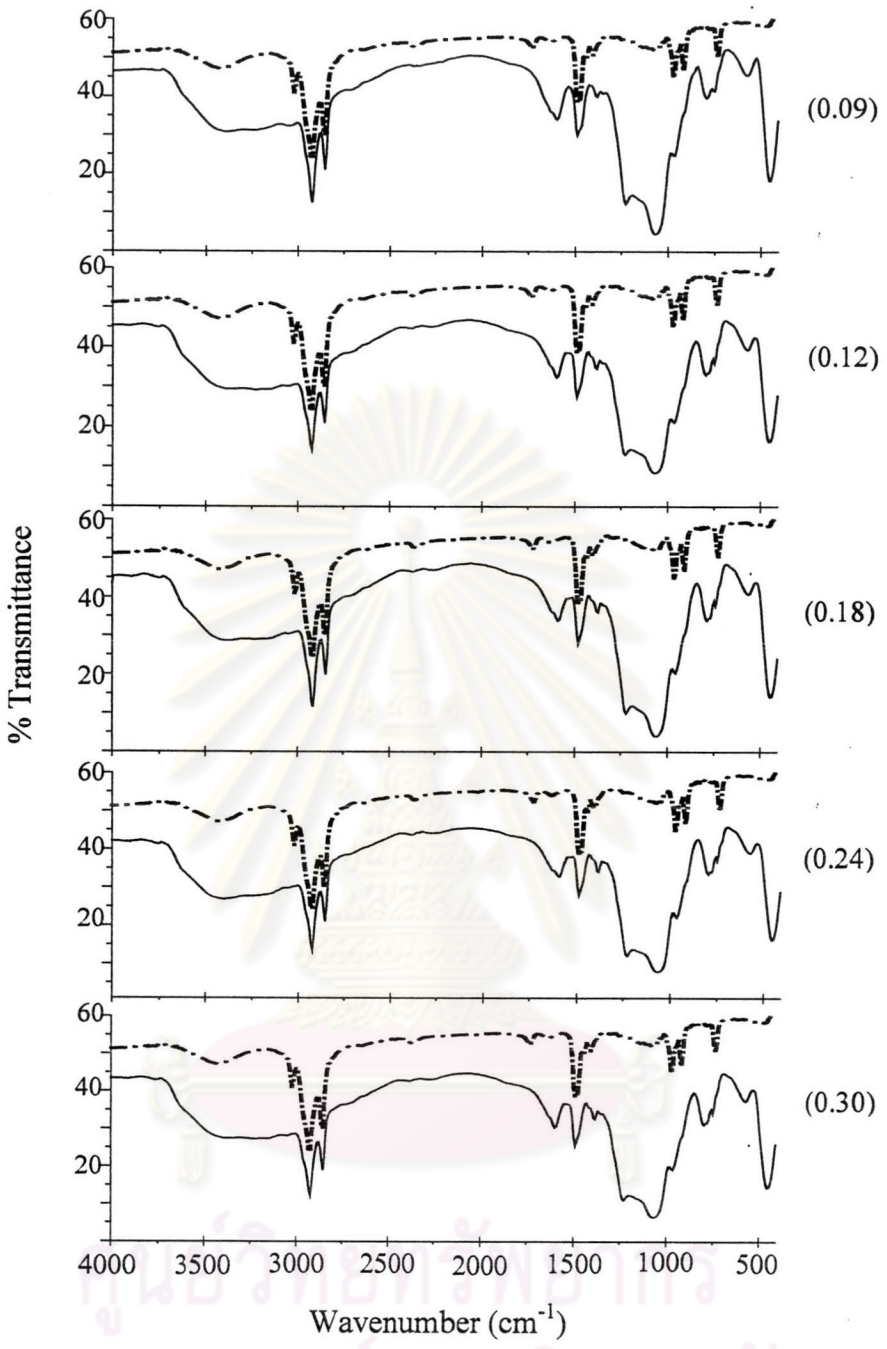

Figure 4.12 FT-IR spectra of non-doped mesoporous silica prepared with various mole ratios of CTAB/TEOS (dash-dot: CTAB, solid: non-doped mesoporous silica).

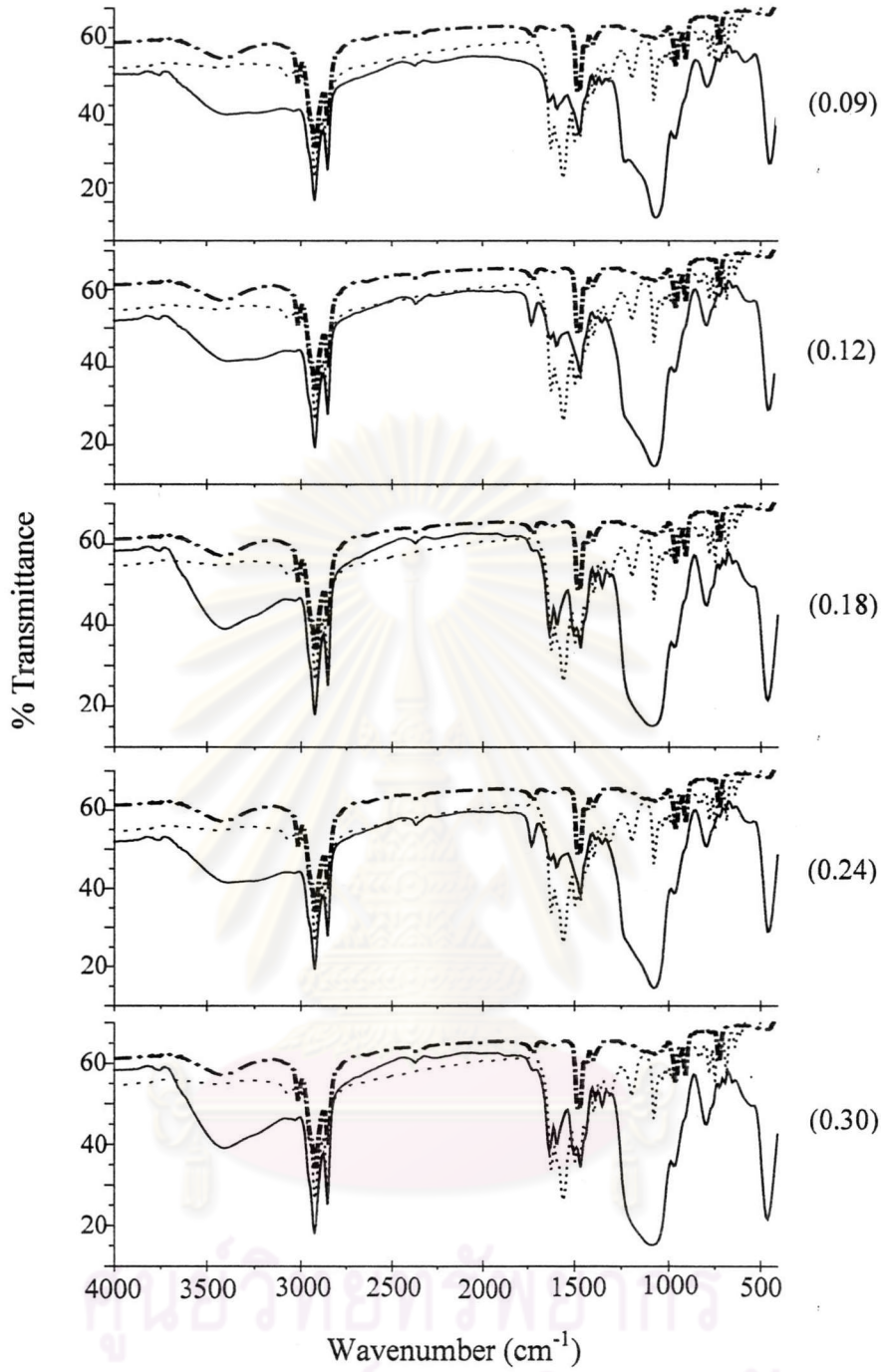

Figure 4.13 FT-IR spectra of HPMSP doped mesoporous silica prepared with various mole ratios of CTAB/TEOS (dash-dot: CTAB, dot: HPMSP, solid: HPMSP doped mesoporous silica).

4.2.2.4. Determination of accessible HPMSP

The accessible HPMSP results of each HPMSP doped mesoporous silica synthesized from different mole ratios of CTAB/TEOS were excellent since all incorporated HPMSP could be extracted out of the silica completely. These results may lead to the profit in the metal extraction properties of this material.

4.2.2.5. Crystallinity of materials

The XRD patterns of each non-doped and HPMSP doped mesoporous silica synthesized from different mole ratios of CTAB/TEOS were shown in Figures 4.14 and 4.15. The d-spacing values of all materials were also summarized in Table 4.12.

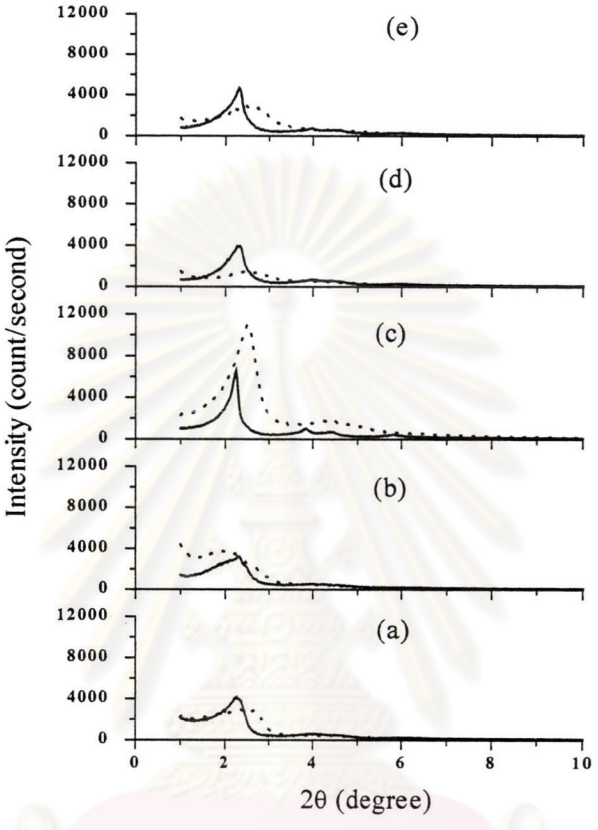

Figure 4.14 XRD patterns of non-doped mesoporous silica synthesized from various CTAB/TEOS mole ratios: (a) 0.09, (b) 0.12, (c) 0.18, (d) 0.24, (e) 0.30 (solid line: as synthesized silica, dot line: calcined silica).

ศูนย์วิทยทรัพยากร
จุฬาลงกรณ์มหาวิทยาลัย

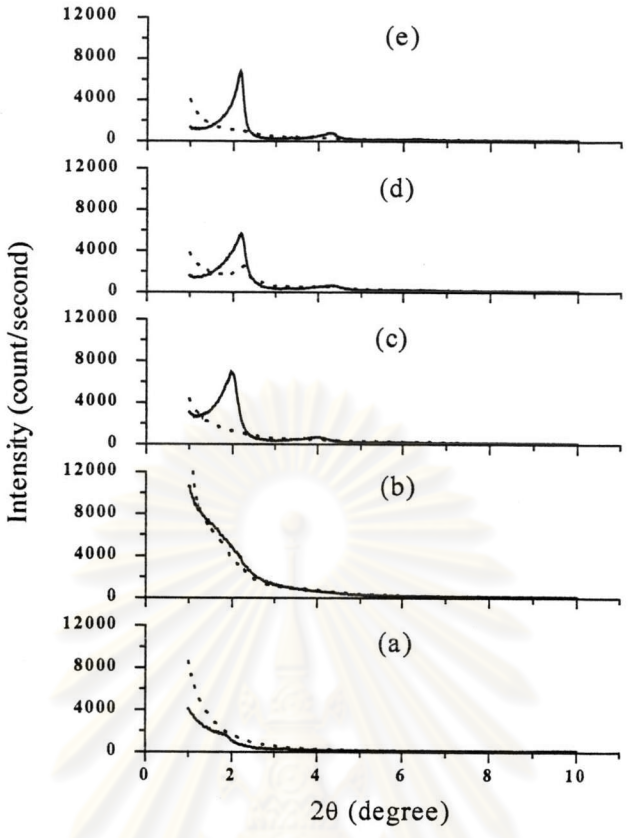

Figure 4.15 XRD patterns of HPMSP-doped mesoporous silica synthesized from various CTAB/TEOS mole ratios: (a) 0.09, (b) 0.12, (c) 0.18, (d) 0.24, (e) 0.30 (solid line: as synthesized silica, dot line: calcined silica).

The XRD patterns of most types of non-doped and HPMSP doped mesoporous silica synthesized from various mole ratios of CTAB/TEOS presented the diffraction peaks which exhibited the crystallinity of the solid structure at 2θ around 2°. On the contrary, the amorphous of HPMSP doped mesoporous silica was observed when the mole ratio of CTAB/TEOS used for the synthesis was less than or equal to 0.12. In addition, for most calcined materials, the diffraction peaks were minimized or absent. These phenomena were probably due to the loss of organic molecules during the calcination process which promoted the collapse of silica's crystalline structure.

For the XRD pattern of the calcined non-doped mesoporous silica synthesized from 0.18 CTAB/TEOS mole ratio, the intensity of this spectrum was found to be higher than that of the as-synthesized sorbent. This observation might be due to better ordering of the inorganic framework or increasing in scattering domain size and thermal stability of the sorbent.

Table 4.12 XRD results of different non-doped and HPMSP doped mesoporous silica synthesized from various mole ratios of CTAB/TEOS.

CTAB/TEOS (mole ratio)	Non-doped mesoporous silica				HPMSP doped mesoporous silica			
	As-synthesized silica		Calcined silica		As-synthesized silica		Calcined silica	
	2θ (degree)	d-spacing (Å)	2θ (degree)	d-spacing (Å)	2θ (degree)	d-spacing (Å)	2θ (degree)	d-spacing (Å)
0.09	2.260 4.060 4.659	39.06 21.74 18.95	2.500	35.31	1.789	49.33	-	-
0.12	1.880 2.281 4.001 4.221	46.94 38.70 22.06 20.91	1.803 2.160 2.670	48.96 40.87 33.06	1.960 4.140	45.02 21.32	-	-
0.18	2.238 3.840 4.381 5.859	39.44 22.98 20.15 15.07	2.500 4.440 4.969	35.31 19.88 17.77	1.960 4.039	45.02 21.85	1.309	67.42
0.24	2.319 3.961 4.480 5.940	38.05 22.28 19.70 14.86	2.460 2.817	35.88 31.33	2.180 4.281	40.49 20.62	2.260 2.609 4.259	39.06 33.82 20.72
0.30	2.300 3.979 4.540 6.025	38.37 22.18 19.44 14.65	2.580	34.21	2.159 4.260 6.379	40.88 20.72 13.84	1.910 2.140 2.459 7.263	46.22 41.24 35.89 12.16

4.2.2.6. Surface area, pore volume and pore size.

The nitrogen sorption isotherm and pore size distribution of HPMSP doped mesoporous silica synthesized from the different mole ratios of CTAB/TEOS were shown in Figures 4.16 and Figure 4.17, respectively. As seen from Figure 4.16, all samples were typical type IV N_2 adsorption-desorption isotherms with H3 and H4 hysteresis loop, indicating uniformly sized mesoporous structure with solid consisted of aggregates or agglomerates of particles forming slit shaped pore. The BJH desorption results from Figure 4.17 confirmed the mesopore of the modified silica with narrow pore size distribution and a mean value of 4-15 nm. Furthermore, the BET surface area, pore volume and mesoporosity were calculated using these isotherms and listed in Table 4.13. From that table, when the mole ratio of CTAB/TEOS used for the synthesis of materials was greater than or equal to 0.12, the surface area of the silica seemed to decrease with the increasing of CTAB/TEOS mole ratio. The average pore diameter of all sorbents confirmed the mesopore of these materials.

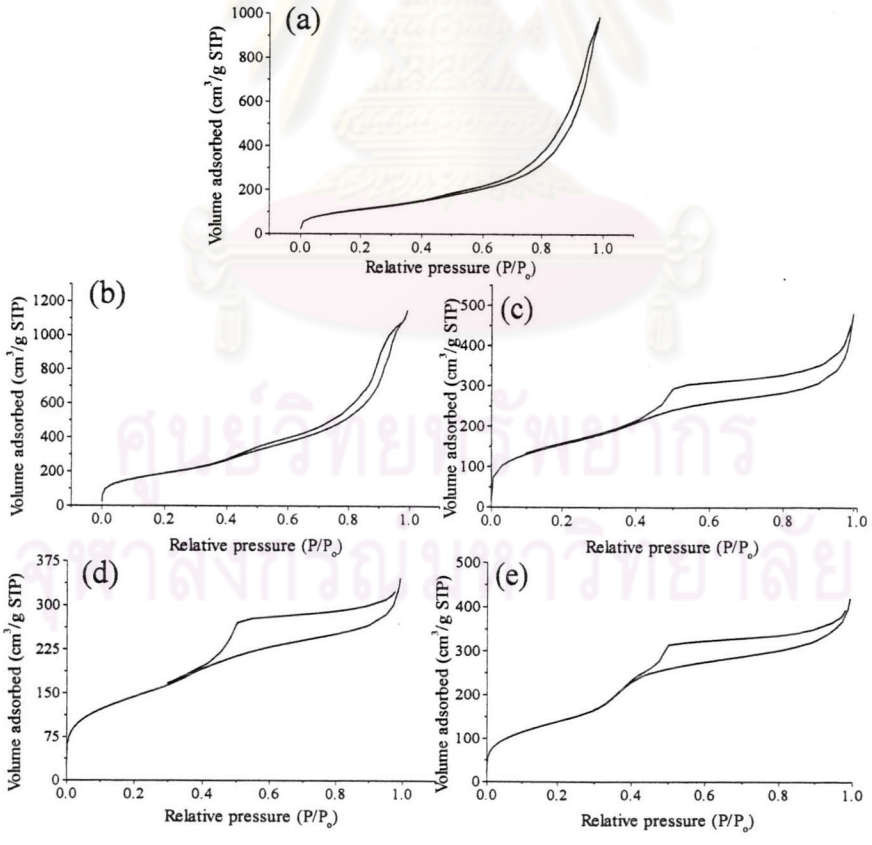

Figure 4.16 Nitrogen sorption isotherms of HPMSP doped mesoporous silica synthesized from various CTAB/TEOS mole ratios: (a) 0.09, (b) 0.12, (c) 0.18, (d) 0.24 and (e) 0.30.

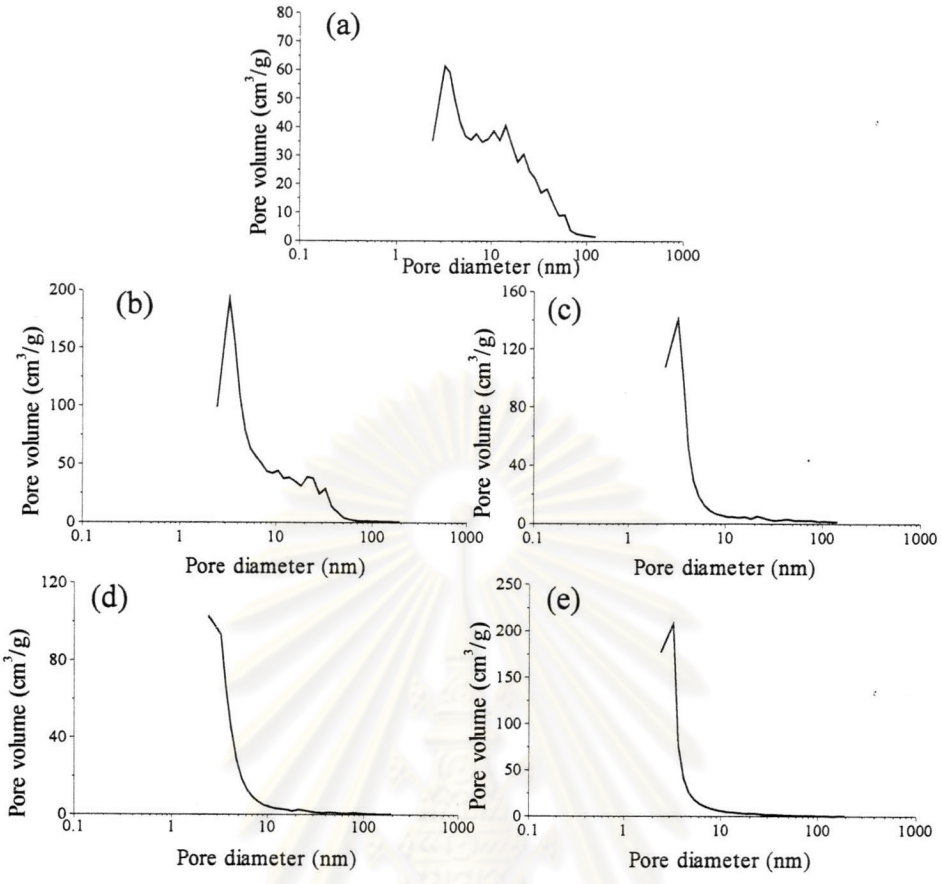

Figure 4.17 BJH pore diameters of HPMSP doped mesoporous silica synthesized from various CTAB/TEOS mole ratios: (a) 0.09, (b) 0.12, (c) 0.18, (d) 0.24 and (e) 0.30.

Table 4.13 Characterization results of calcined HPMSP-doped mesoporous silica synthesized from various mole ratios of CTAB/TEOS determined from N_2 sorption experiment at 77 K and XRD measurement.

CTAB/TEOS (mole ratio)	S (m^2/g)	Vp (cm^3/g)	APD (nm)	d_{100} (nm)	a_0 (nm)	w (nm)
0.09	392	1.52	15.51	-	-	-
0.12	663	1.76	10.62	-	-	-
0.18	550	0.74	5.38	6.74	23.34	17.96
0.24	507	0.52	4.10	3.91	13.54	9.44
0.30	483	0.63	5.21	4.12	14.27	9.06

S, BET surface area (m^2/g) obtained from N_2 sorption; V_p, Total pore volume (cm^3/g) obtained from single-point volume at $P/P_o = 0.99$; APD, average pore diameter calculated from $4Vp/S$; d_{100}, d-value 100 reflections; a_o = the lattice parameter, from the XRD data using the formula $a_o = 2d_{100}\sqrt{3}$; w, pore wall thickness was equaled to a_o-APD.

Considering the pore wall thickness of silica, it was found that the material synthesized from 0.18 CTAB/TEOS mole ratio had the highest pore wall thickness. This result indicated the stability of this sorbent during the calcination process.

4.2.2.7. Morphology of materials

The micro structural feature of HPMSP modified material synthesized from different mole ratios of CTAB/TEOS was investigated. The results were shown in Figure 4.18. The SEM micrographs showed the spherical shape of all silica particles with some aggregates. It is also noteworthy that the aggregate particles were minimized when the material was synthesized using the mole ratio of CTAB/TEOS equal to 0.18. The particle sizes of all HPMSP modified sorbents were varied from 10 to 28 μm as tabulated in Table 4.14.

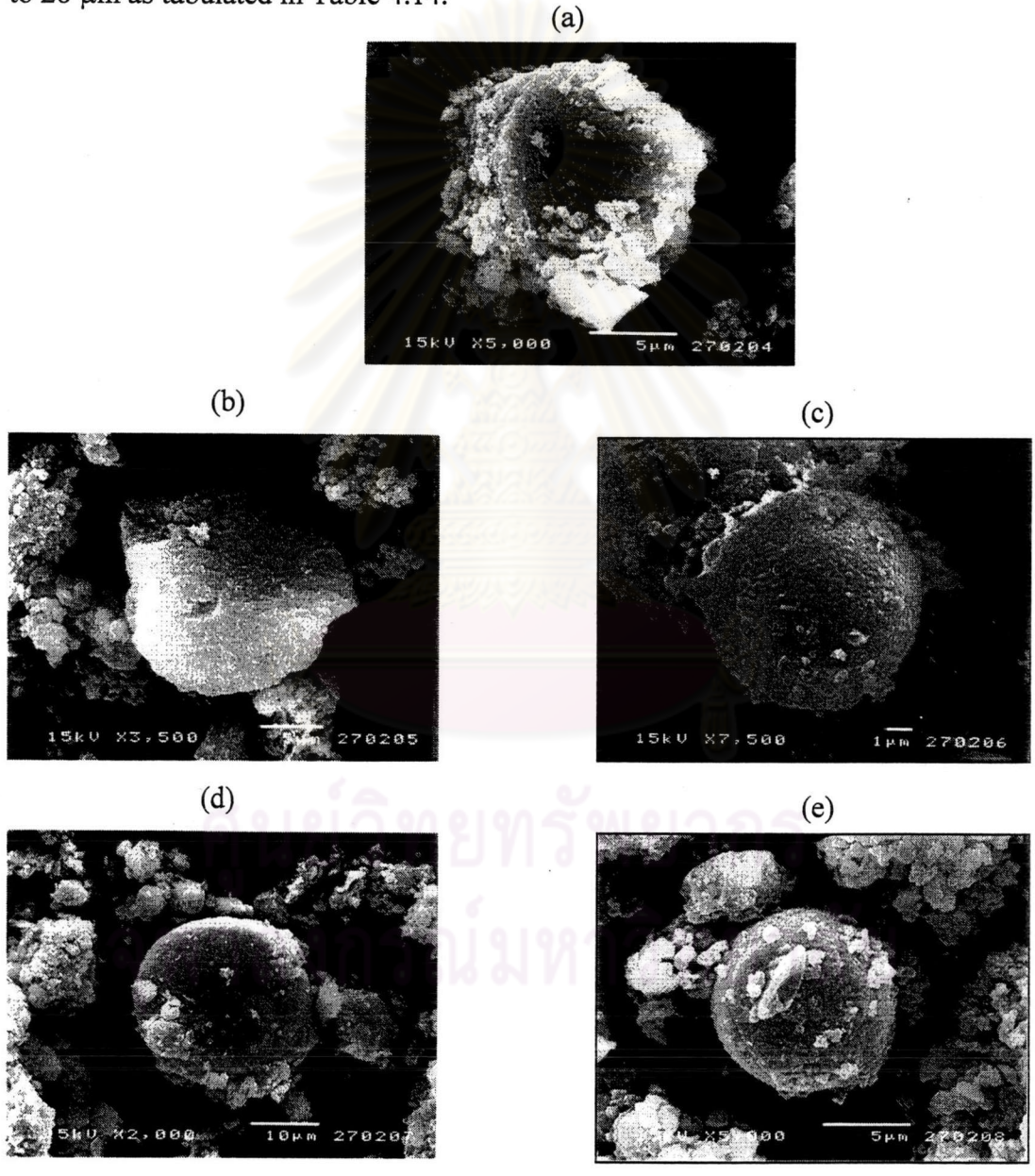

Figure 4.18 SEM images of HPMSP doped mesoporous silica prepared with different mole ratios of CTAB/TEOS: (A) 0.09, (B) 0.12, (C) 0.18, (D) 0.24 and (E) 0.30.

Table 4.14 The particle size of mesoporous silica synthesized from different mole ratios of CTAB/TEOS.

CTAB/TEOS	Particle size (μm)
0.09	11.67
0.12	16.67
0.18	10.00
0.24	27.78
0.30	10.83

4.2.2.8. Particle size

The particle size of HPMSP doped mesoporous silica synthesized from different mole ratios of CTAB/TEOS was determined using the Malvern laser diffraction technique. The representative particle size curves of these materials based on volume were exhibited in Figure 4.19 and the frequently found particle sizes of each material were summarized in Table 4.15.

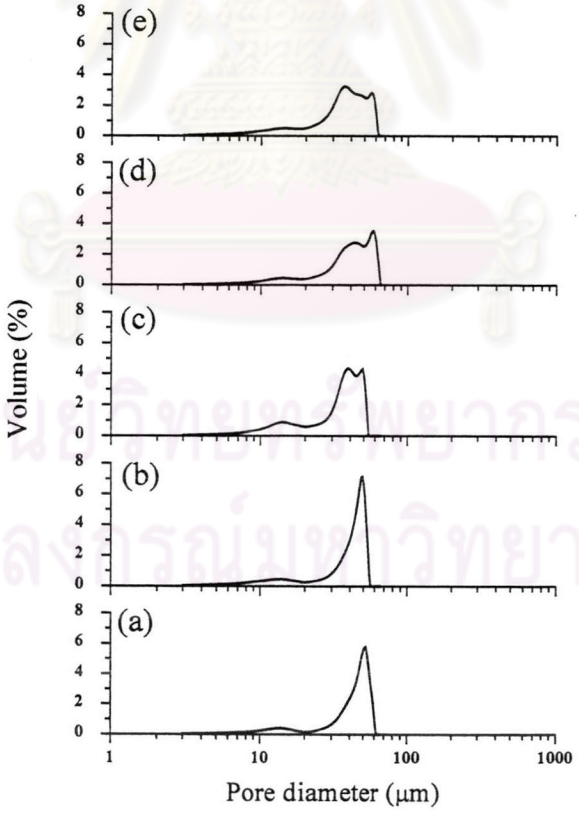

Figure 4.19 Particle diameters of HPMSP doped mesoporous silica prepared with various mole ratios of CTAB/TEOS: (a) 0.09, (b) 0.12, (c) 0.18, (d) 0.24 and (e) 0.30.

From the experimental results shown below, it could be seen that the particle size distribution of HPMSP doped mesoporous silica was narrow when the mole ratios of CTAB/TEOS used for the synthesis of these materials was less than 0.12. On the contrary, when the mole ratio of CTAB/TEOS used for the synthesis was more than 0.18, the particle size distribution of materials was fairly broad. In these cases, two frequently found particle sizes of materials were observed. These results implied that the amounts of CTAB used for the synthesis had a crucial role for the obtained particle sizes of the sorbent.

Table 4.15 The frequently found particle sizes of HPMSP doped mesoporous silica prepared with various mole ratios of CTAB/TEOS

CTAB/TEOS	Particle size (μm)
0.09	96.25
0.12	56.56
0.18	13.22 and 52.66
0.24	24.35 and 240.62
0.30	8.36 and 190.03

4.2.3. Cu(II) extraction properties of materials

The Cu(II) extractabilities of HPMSP doped mesoporous silica synthesized from different mole ratios of CTAB/TEOS were determined using batch and SPE column method. The key parameters such as flow rate, sample volume and initial metal concentration were optimized. The Cu(II) solution containing 0.1 M $NaNO_3$ at pH 2 with the initial concentration of 200 ppm was used as metal ion studied and the dose of sorbent was 0.2 g. The extraction experiments were performed in triplicate and the results were shown as follows.

4.2.3.1. Batch method

The relation between the Cu(II) extractability of HPMSP modified sorbents and the mole ratio of CTAB/TEOS used for the synthesis was displayed in Figure 4.20. As seen, the amounts of Cu(II) extracted seemed to decrease exponentially as a function of CTAB/TEOS mole ratio. These results may be caused by an excess of free CTAB molecules in the modified sorbents [29]. Indeed, the more positive charge, which was augmented with the increasing of CTAB/TEOS mole ratio, created by the

free CTAB molecules on the silica surface, the more repulsion of metal ions was occurred. Consequently, the Cu(II) extraction was decreased.

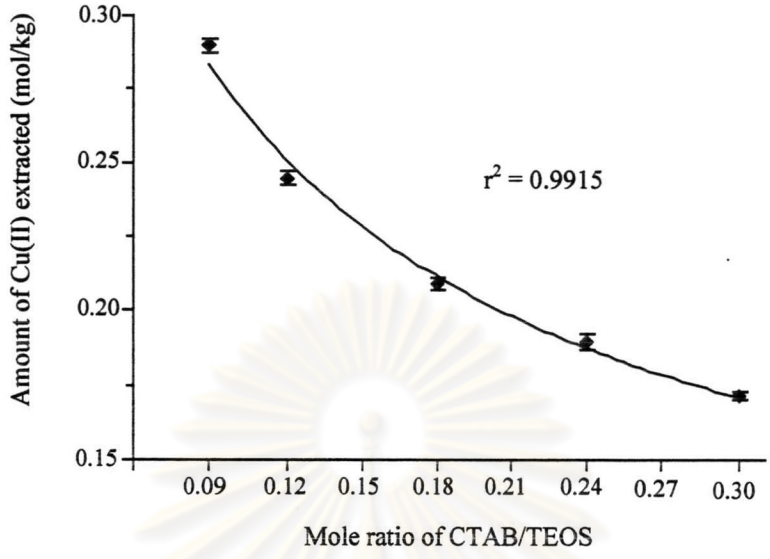

Figure 4.20 Amounts of Cu(II) extracted by different HPMSP modified sorbents synthesized from various mole ratios of CTAB/TEOS.

4.2.3.2. SPE column method

In general, the metal ions in an environmental sample are often present in trace level. Therefore, prior to metal determination the preconcentration of such metal ions is necessary. The extraction of elements using SPE column method is among the popular methods to support this purpose. This technique has many advantages such as low consumption of solvent, rapidity of extraction time and minimum waste generation. In this work, the extraction of Cu(II) by HPMSP doped mesoporous silica was also investigated by SPE column method. The flow rate of 1 mL/min was maintained for the whole experiment. The extraction was performed in triplicate. The Cu(II) extraction efficiency results of different HPMSP doped mesoporous silicas synthesized from various mole ratios of CTAB/TEOS were displayed in Figure 4.21.

As seen from Figure 4.21, the amounts of Cu(II) extracted seemed to increase proportionally as a function of the mole ratio of CTAB/TEOS used for the synthesis. However, the reason for these observations is still not clear to us. Indeed, the more positive charge, which was augmented with the increasing of CTAB/TEOS mole ratio, created by the free CTAB molecules on the silica surface, the more repulsion of metal ions was occurred. And in SPE column method the time of interaction between

metal ions and CTA^+ was limited, thus the effect of CTA^+ on the Cu(II) extraction was probably minimal.

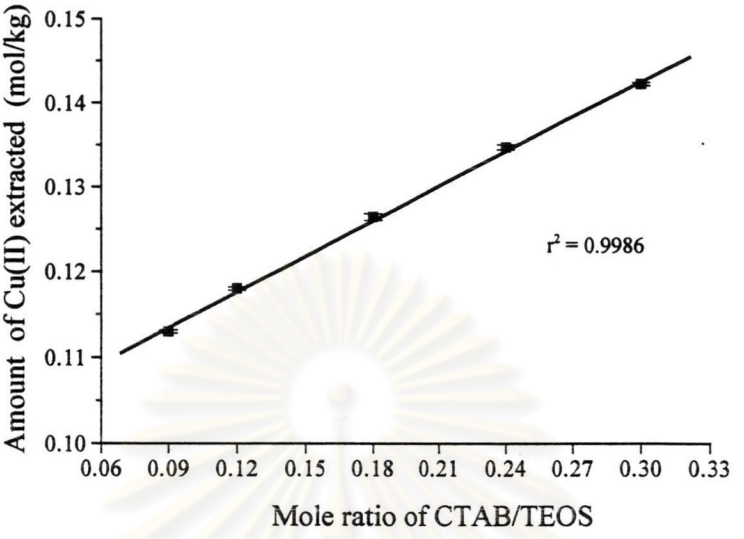

Figure 4.21 Amounts of Cu(II) extracted by different HPMSP modified sorbents synthesized from various mole ratios of CTAB/TEOS.

The comparison between the amounts of Cu(II) extracted by SPE column method and those by batch method was shown in Table 4.16. It was found that the Cu(II) extracted values obtained from SPE column method were lower than those of batch method. However, the column method provided the short operating time of extraction process which made the analytical procedure reasonably fast. Moreover, the amounts of Cu(II) extracted by this dynamic method were still satisfactory. Thus, this technique was further applied for the preconcentration of trace metals contained in real samples.

Table 4.16 Amounts of Cu(II) extracted by HPMSP doped mesoporous silica synthesized from various mole ratios of CTAB/TEOS using SPE column and batch method.

CTAB/TEOS (mole ratio)	Cu(II) extracted (mol/kg)	
	SPE column method	Batch method
0.09	0.1099 ± 0.0002	0.2887 ± 0.0011
0.12	0.1180 ± 0.0002	0.2431 ± 0.0020
0.18	0.1264 ± 0.0004	0.2090 ± 0.0022
0.24	0.1347 ± 0.0003	0.1850 ± 0.0066
0.30	0.1423 ± 0.0002	0.1633 ± 0.0113

(i) Reproducibility of adsorption

The reproducibility of each sorbent synthesized from different mole ratios of CTAB/TEOS for the extraction of Cu(II) was investigated in 15 replicates using the same metal solution medium as stated previously. The results were tabulated in Table 4.17.

Table 4.17 The amounts of Cu(II) extracted by different HPMSP modified sorbents synthesized from various mole ratios of CTAB/TEOS.

Extraction number	Amount of Cu(II) extracted (mol/kg) by each silica				
	0.09*	0.12*	0.18*	0.24*	0.30*
1	0.1077	0.1156	0.1238	0.1313	0.1396
2	0.1074	0.1159	0.1240	0.1335	0.1405
3	0.1088	0.1165	0.1252	0.1329	0.1409
4	0.1125	0.1202	0.1292	0.1364	0.1446
5	0.1113	0.1195	0.1277	0.1351	0.1433
6	0.1112	0.1196	0.1278	0.1373	0.1442
7	0.1087	0.1169	0.1249	0.1325	0.1406
8	0.1086	0.1170	0.1249	0.1346	0.1413
9	0.1115	0.1192	0.1281	0.1353	0.1436
10	0.1115	0.1192	0.1281	0.1353	0.1436
11	0.1102	0.1187	0.1266	0.1363	0.1432
12	0.1086	0.1170	0.1251	0.1345	0.1413
13	0.1111	0.1189	0.1277	0.1349	0.1434
14	0.1099	0.1183	0.1262	0.1359	0.1428
15	0.1098	0.1182	0.1264	0.1357	0.1427
Average	0.1100	0.1181	0.1265	0.1349	0.1425
S.D.	0.0016	0.0015	0.0017	0.0016	0.0015
% RSD	1.45	1.27	1.34	1.19	1.05

* These number were the mole ratio of CTAB/TEOS used for the synthesis of each modified silica.

As could be seen from Table 4.17 that the relative standard deviation of Cu(II) extracted by all HPMSP doped mesoporous silica was small, so these modified materials possess an excellent reproducibility of extraction towards the Cu(II) ions.

(ii) Desorption

One of the advantages of sorbents is their reusability. However, prior to reuse the sorbent, the former analytes should be removed as much as possible. Thus, in this study, the adsorbed Cu(II) is eluted from the silica by nitric acid. This acid was chosen since the nitrate ions were an acceptable matrix for flame AAS experiment. The eluent concentration was varied between 0.5 to 1.0 M and the volume of nitric acid used was 5 mL and 10 mL. The Cu(II) desorption efficiency of various sorbents synthesized from different mole ratios of CTAB/TEOS were displayed in Figure 4.22.

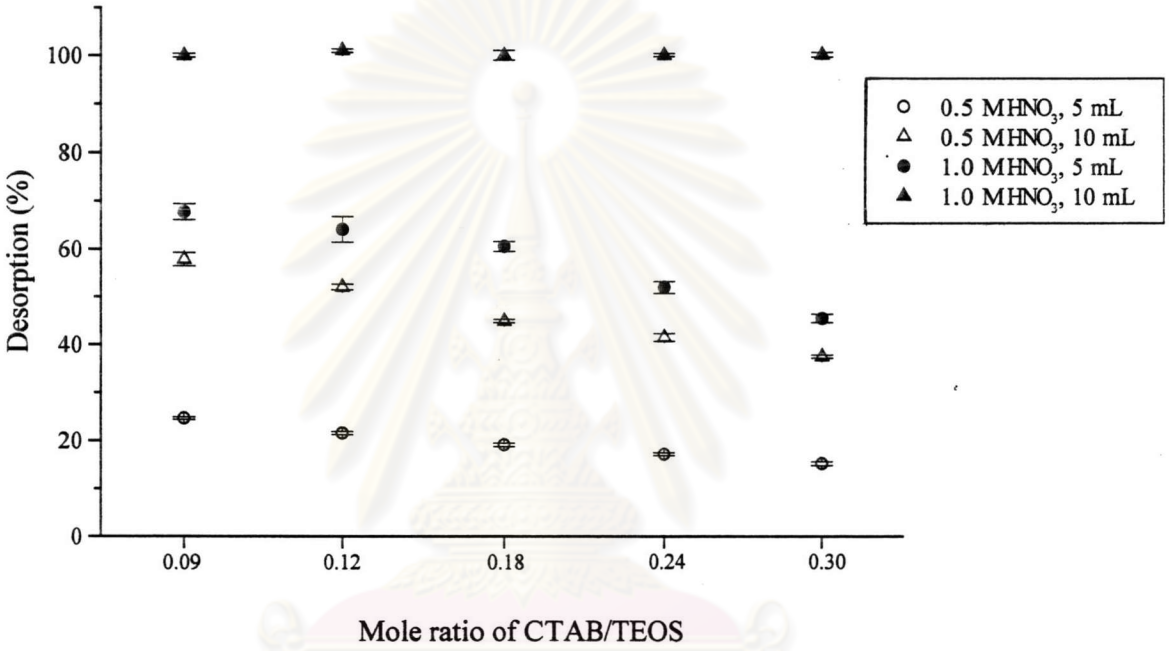

Figure 4.22 The Cu(II) desorption efficiency of various HPMSP modified sorbents using different volumes and concentrations of eluent.

As seen, for the entire desorption condition studied, the Cu(II) desorption efficiency of the HPMSP modified sorbents seemed to decrease with the increasing of the mole ratio of CTAB/TEOS used for the synthesis of materials. The Cu(II) ions were completely released from the doping materials when 10 mL of 1.0 M HNO_3 was applied. This condition was then chosen as an eluent for further desorption experiments. In addition, with the materials synthesized from less than 0.18 CTAB/TEOS mole ratio, we encountered the problem of controlling their elution flow rate at 1 mL/min. Thus, due to the synthesis facility, the excellent morphology and the adsorption-desorption efficiency of materials, the HPMSP doped mesoporous silica synthesized from 0.18 CTAB/TEOS mole ratio had been a selective sorbent for further study in details.

4.3. Profound study on the Cu(II) extraction properties of an appropriate sorbent using SPE column method.

From previous sections, the HPMSP doped mesoporous silica synthesized from 0.18 CTAB/TEOS mole ratio had shown the excellent extraction properties due to its high surface area and crystalline structure. Furthermore, the synthesis of this material was facile. Thus, this silica was selected as a sorbent for profound extraction experiments by SPE column method. The Cu(II) solution in 0.1 M $NaNO_3$ medium at pH 2 was used as target metal due to the strong selectivity between this ion and the HPMSP molecules. Several parameters including flow rate, sample volume and initial metal concentration were investigated. The detail of each parameter was described as folllow.

4.3.1. Effect of flow rate

The extraction and elution experiments were performed according to the method described in section 3.3.3.2. The flow rate used in this experiment was varied in the range of 1 to 4 mL/min. The flow rate below 1 mL/min was unfavourable because of long extraction time. The results of flow rate effect on the extraction capacity of HPMSP modified sorbent were summarized in Table 4.18.

Table 4.18 Effect of flow rate on the Cu(II) extraction and elution properties of HPMSP modified sorbent synthesized from 0.18 CTAB/TEOS mole ratio.

Flow rate (mL/min)	Extraction (mol/kg)	Elution (%)
1	0.1263 ± 0.0018	101.54 ± 0.33
2	0.1261 ± 0.0005	100.64 ± 0.48
3	0.1256 ± 0.0007	100.68 ± 0.51
4	0.1249 ± 0.0005	101.07 ± 0.48

From Table 4.18, the extraction of Cu(II) by HPMSP modified silica seem to be decreased when the loading flow rate was greater than 2 mL/min. However, these flow rates did not have any affect on the elution of Cu(II) from the sorbent. Thus, for practical usage and reduction of analysis time, the flow rate of 2 mL/min was selected for further column experiments.

4.3.2. Effect of sample volume on the Cu(II) extraction

In general, the amounts of metal ions present in environmental samples were in a trace level. To determine the trace elements in these samples, the preconcentration of metal ions is thus required prior to analysis. Oftenly, the maximum sample volume is passed through the column to obtain the highest preconcentration factor. Thus, in this study, the effect of sample volume on the Cu(II) extraction behavior of materials was examined. The range of volume of Cu(II) solution loaded into the SPE column was from 25 mL to 45 mL at 5-mL intervals. The flow rate of 2 mL/min was used for the whole experiment. The Cu(II) extracted values as a function of sample volume were shown in Figure 4.23. It was found that the Cu(II) extractability of the sorbent was not affected by the sample volume loaded for the entire range studied. However, when considering the relation between the sample volume and the Cu(II) extraction efficiency shown in Figure 4.24, it was found that the percentage extraction at equilibrium decreased with the increasing of sample volume. This meant that the HPMSP modified silica was probably already saturated when the volume of Cu(II) loaded was 25 mL Consequently, it could not retain additional Cu(II) ions when much more sample volume was applied.

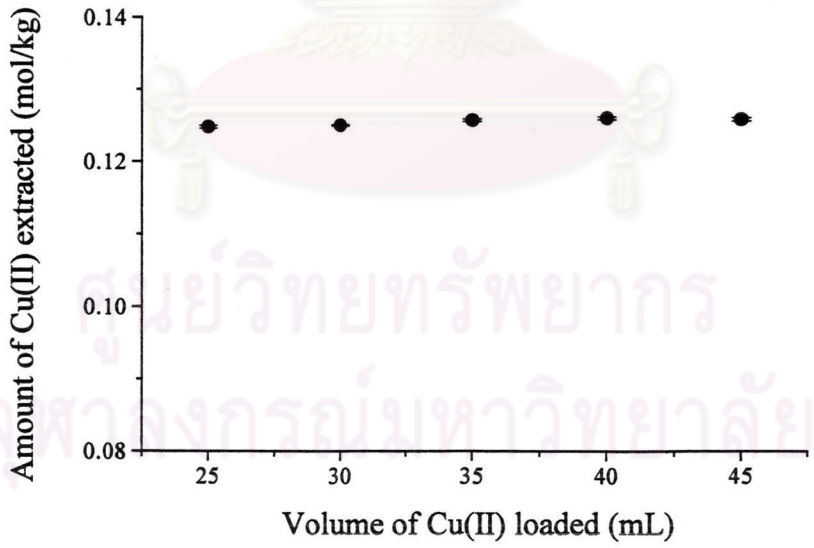

Figure 4.23 Effect of sample volume on the Cu(II) extraction efficiency of HPMSP modified sorbent.

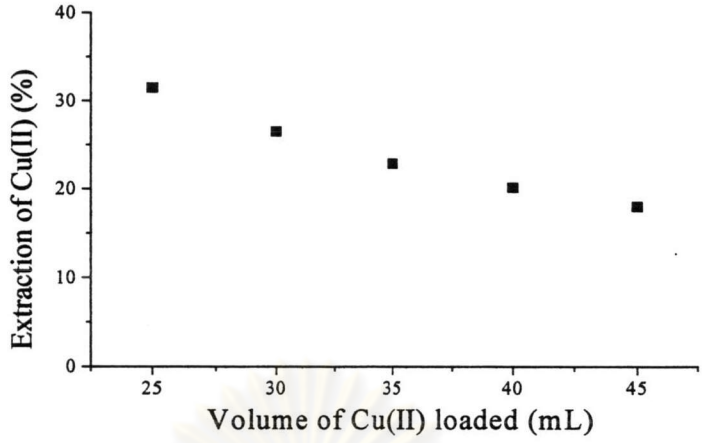

Figure 4.24 Relation between the percentage extraction of Cu(II) at equilibrium and the volume of Cu(II) loaded.

4.3.3. Determination of column capacity

The capacity of sorbent is an important factor to determine how much sorbent is required to quantitatively remove a specific amount of metal ions from the solution. In this work, the column capacity of HPMSP doped mesoporous silica was examined using Cu(II) solution in 0.1 M $NaNO_3$ medium at pH 2 and the range of Cu(II) concentration was varied from 100 ppm to 400 ppm. The flow rate used through the experiments was 2 mL/min. The obtained results were shown in Figure 4.25.

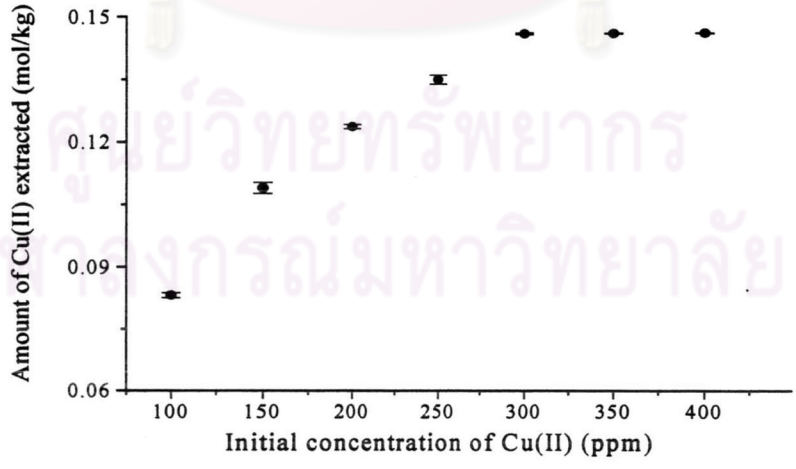

Figure 4.25 Effect of initial concentration on the Cu(II) extraction capacity of HPMSP doped mesoporous silica.

From Figure 4.25, the Cu(II) extractability of HPMSP modified silica seemed to increase with the increasing of initial concentration of Cu(II) and reached a plateau when the concentration of Cu(II) was ≥ 300 ppm. The adsorption isotherm type of the sorbent could be determined by plotting the amounts of Cu(II) extracted (N_f) against the concentration of Cu(II) at equilibrium (C_e). The obtained profile shown in Figure 4.26 (a) gave best fit for the Langmuir model.The maximum extraction capacity of the sorbent (N_s) which could be calculated from the slope of the straight line obtained from the plot of C_e/N_f versus C_e as shown in Figure 4.26 (b), was found to be 11.21 mg/g (0.1764 mol/kg). Also, the equilibrium constant of the extraction (K_L) calculated from the intercept of the Langmuir plot was found to be 0.0169 mL/mg. This value was superior to Cu(II) extraction capacity of other functionalized sorbents reported elsewhere (i.e. 0.0780 mol/kg for zirconium phosphate functionalized silica [42] and 0.1561 mol/kg for octadecyl silica membrane disks modified by glyoxime derivative [37]).

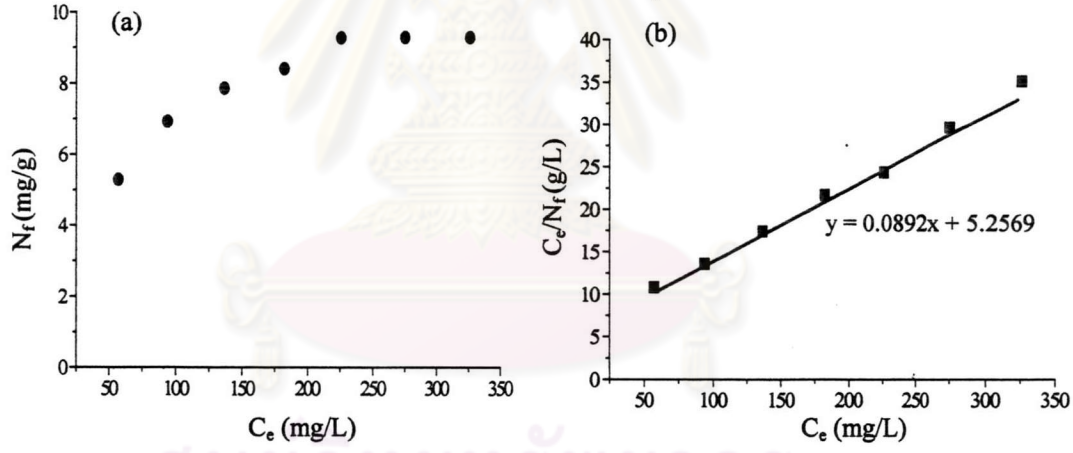

Figure 4.26 (a) Adsorption isotherm of Cu(II) on HPMSP doped mesoporous silica obtained from column method and (b) Linearization of the adsorption isotherm.

4.3.4. Reproducibility

The reproducibility of the Cu(II) extraction by HPMSP doped mesoporous silica synthesized from the mole ratio of CTAB/TEOS equal to 0.18 was also performed using column method with a flow rate of 2 mL/min. The results obtained from five experiments were tabulated in Table 4.19. It was evident that this HPMSP modified material had excellent extraction reproducibility since the percentage of the relative standard deviation was relatively low.

Table 4.19 The amounts of Cu(II) extracted in different experiments by HPMSP doped mesoporous silica.

Experiment number	Amounts of Cu(II) extracted (mol/kg)
1	0.1263
2	0.1263
3	0.1260
4	0.1260
5	0.1256
Average	0.1260
S.D.	0.0003
% RSD	0.24

4.3.5. Reusability

The reusability of sorbent is one of the major objective for most researches concerning the development of sorbent because it can reduce the cost of sample separation and waste disposal. To demonstrate the potential reusability of HPMSP modified silica, this sorbent was then subjected to several adsorption-desorption experiments. The adsorption was carried out by loading 25 mL of 200 ppm of Cu(II) in 0.1 M $NaNO_3$ medium at pH 2 and the desorption was performed using 10 mL of 1.0 M HNO_3 as elution agent. The Cu(II) adsorption-desorption cycle was repeated five times on the same sorbent. The flow rate was maintained at 2 mL/min for the whole experiment. The results of each cycle were summarized in Table 4.20.

Table 4.20 The amounts of Cu(II) adsorbed and desorbed on the HPMSP modified sorbent from each extraction cycle.

Cycle number	Amounts of Cu(II)	
	Adsorption (mol/kg)	Desorption (%)
1	0.1263 ± 0.0013	100.42 ± 0.50
2	0.1263 ± 0.0013	100.49 ± 0.53
3	0.1260 ± 0.0012	100.76 ± 0.51
4	0.1260 ± 0.0007	100.41 ± 0.32
5	0.1256 ± 0.0017	100.85 ± 0.76

From Table 4.20, no change in the sorption capacity of the HPMSP modified silica was observed even after five cycles of adsorption-desorption. The Cu(II) uptake obtained in the first sorption cycle was reached again in any of the subsequent cycles. The percentage desorption was also totally accomplished for all cycles. On account of its reusability, this sorbent was thus a promising candidate for large scale application.

4.4. Application of the appropriate HPMSP doped mesoporous silica to the extraction of other metal ions

Apart from the extraction of Cu(II), the HPMSP doped mesoporous silica synthesized with 0.18 CTAB/TEOS mole ratio was also applied to the extraction of other metal ions such as Zn(II), Fe(III) and Mn(II). Various parameters influenced the extractability of the modified sorbent were investigated in both batch and column methods. The results of each method were described below.

4.4.1. Batch method

4.4.1.1. Reproducibility

The reproducibility of HPMSP doped mesoporous silica towards the metal extraction was examined using 200 ppm of Zn(II) solution in 0.1 M $NaNO_3$ medium at pH 3 as metal solution. The non-doped mesoporous silica synthesized from the same mole ratio of CTAB/TEOS was also served as comparative sorbent for this study. The extraction experiments were repeated nine times and their results were shown in Table 4.21.

Table 4.21 The amounts of Zn(II) extracted by non-doped and HPMSP doped mesoporous silica synthesized with 0.18 CTAB/TEOS mole ratio.

Extraction number	Amounts of Zn(II) extracted (mol/kg)	
	Non-doped silica	HPMSP doped silica
1	0.2610	0.3085
2	0.2754	0.3251
3	0.2897	0.3349
4	0.2678	0.3193
5	0.2859	0.3362
6	0.2856	0.3351
7	0.2906	0.3378
Average	0.2805	0.3297
S.D.	0.0118	0.0101
% RSD	4.17	3.05

As seen from Table 4.21, the reproducibility of both sorbents to the extraction of Zn(II) appeared rather good since the percentage of the relative standard deviation was low. Considering the Zn(II) extractability of both sorbents, it was found that the HPMSP modified silica had better Zn(II) extraction efficiency than that of non-doped mesoporous material. This phenomenon might be explained by the association complexes formed between HPMSP molecules and the metal ions.

4.4.1.2. Effect of amounts of silica

One of the key parameters in the evaluation of the metal extraction was the amounts of sorbent. In order to elucidate the influence of this parameter, the experiment was carried out using 200 ppm of Zn(II) solution in 0.1 M $NaNO_3$ at pH 3 as a metal solution and the amounts of non-doped and HPMSP doped mesoporous silica were varied from 0.025 to 0.200 g. The extracted values of Zn(II) ions by both sorbents were presented in term of adsorbent dose profile versus the Zn(II) extracted values as displayed in Figure 4.27.

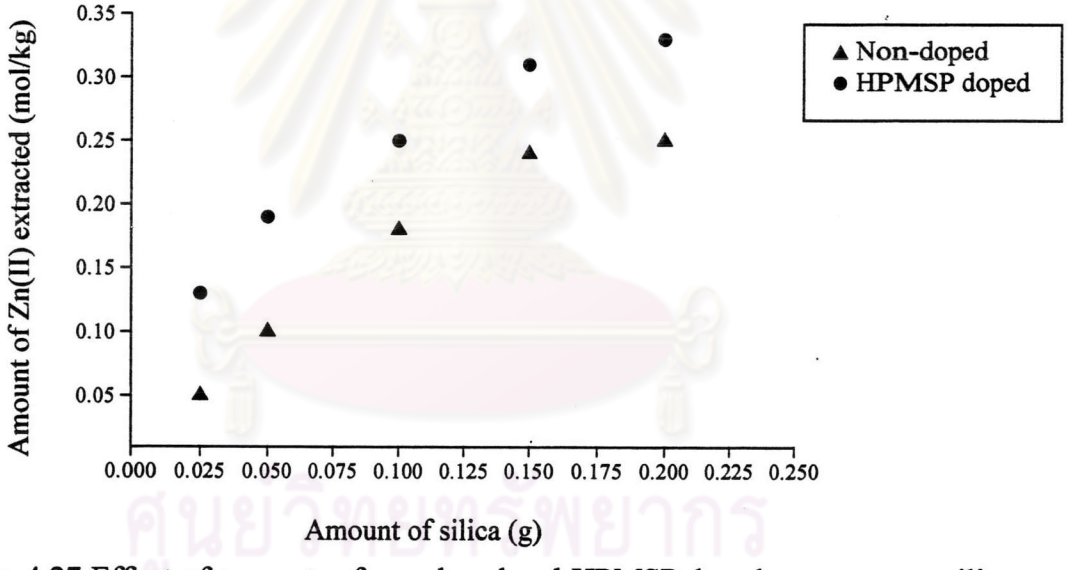

Figure 4.27 Effect of amounts of non-doped and HPMSP doped mesoporous silica on the extraction of Zn(II).

It could be observed from Figure 4.27 that on increasing the adsorbent dose the Zn(II) extracted values were enhanced sharply and reached its maximum value when the amount of sorbents was more than 0.15 g. Furthermore, the amounts of Zn(II) extracted by the HPMSP modified sorbents were higher than those of non-doped silica for the whole range of silica extent studied. These results may be explained by the same reason as described previously in 4.4.1.1.

4.4.1.3. Determination of Zn(II) extractability of silica

The Zn(II) extractability of non-doped and HPMSP doped mesoporous silica was determined using the Zn(II) solution in 0.1 M $NaNO_3$ medium with the concentration of Zn(II) varied from 100 to 300 ppm. The results were displayed in Figure 4.28. As seen, the plots between the amounts of Zn(II) extracted by both sorbents and the initial concentration of Zn(II) were continuous curves leading to saturation when the concentration of Zn(II) was greater than or equal to 200 ppm. These results suggested the possible monolayer coverage of Zn(II) on the surface of the sorbents. In fact, at lower metal concentration, the ratio of number of moles of Zn(II) in solution to the available surface area was low and hence the adsorption was dependent on the initial concentration. On the contrary, at higher concentration the available sites of the sorbent for adsorption were less and hence the metal extraction was independent of the initial metal concentration.

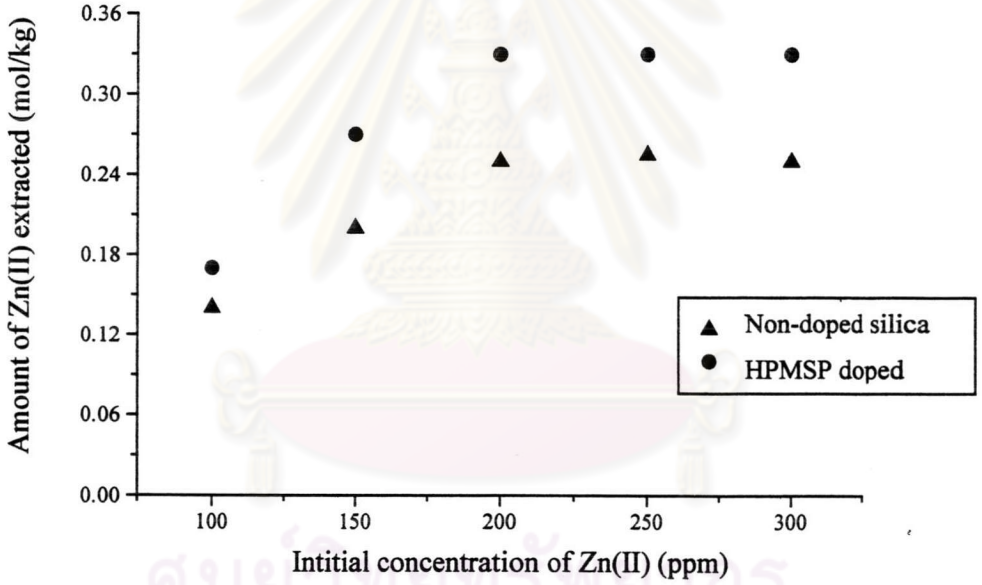

Figure 4.28 Effect of initial concentration on the Zn(II) extraction efficiency of non-doped and HPMSP modified silicas.

To investigate the adsorption isotherm type of both materials, the amounts of Zn(II) extraction (N_f) were plotted against the concentration of Zn(II) at equilibrium (C_e) as shown in Figure 4.29 (a) and 4.30 (a) for non-doped and HPMSP doped mesoporous silica, respectively. From those figures, both obtained profiles gave best fit for the Langmuir model. The maximum extraction capacity (N_s) and the equilibrium constant (K_L) of both sorbents could be determined by considering the plot of C_e/N_f versus C_e as shown in Figure 4.29 (b) and 4.30 (b). Their results were tabulated in Table 4.22. As seen again from that table, the Zn(II) extractability of

HPMSP modified silica was greater than that of non-doped mesoporous silica. This result may be due to the presence of chelating ligand inside the HPMSP modified silica. In addition, the Zn(II) extraction efficiency of both sorbents in this study was relatively greater than that of other functionalized silica (i.e. 0.18 mol/kg for 1,8-dihydroxyanthraquinone modified silica [43] and 0.2200 mol/kg for 2-aminomethylpyridine molecule grafted silica gel [44]).

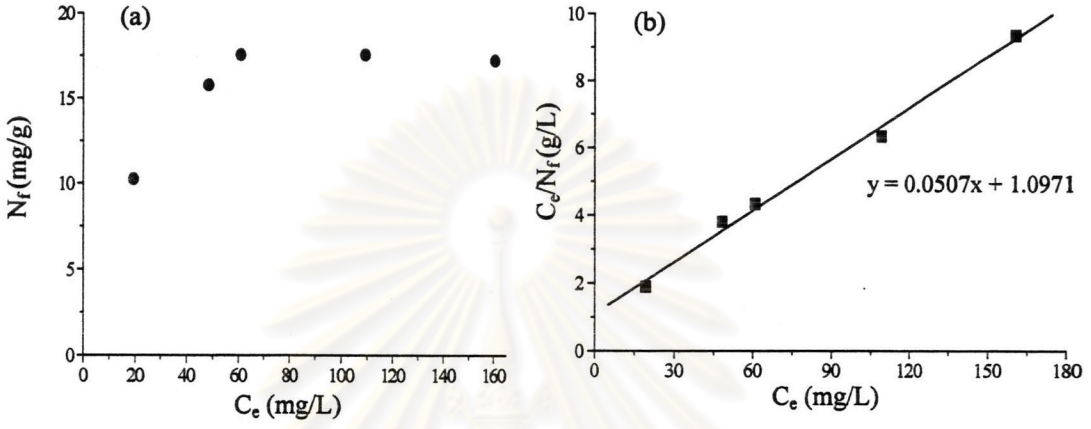

Figure 4.29 (a) Adsorption isotherm of Zn(II) on non-doped mesoporous silica and (b) Linearization of the adsorption isotherm.

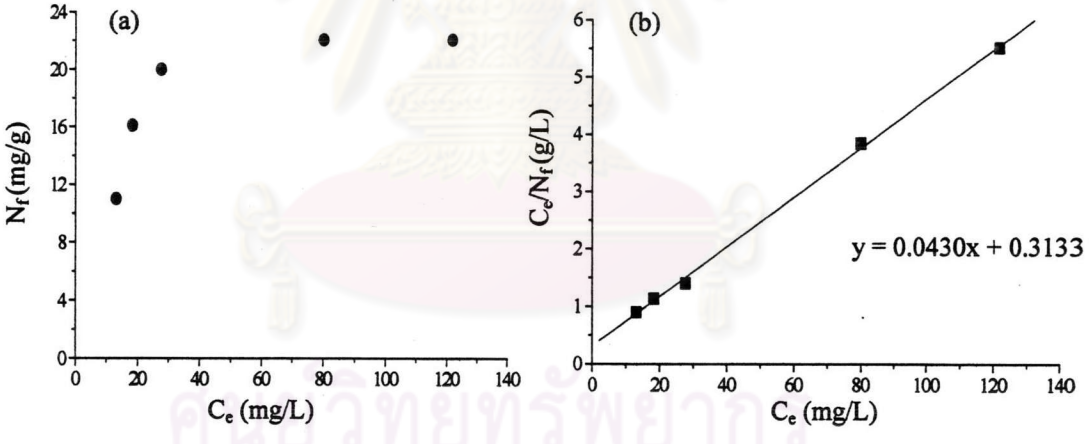

Figure 4.30 (a) Adsorption isotherm of Zn(II) on HPMSP doped mesoporous silica and (b) Linearization of the adsorption isotherm.

Table 4.22 The maximum extraction capacities and equilibrium constants of non-doped and HPMSP doped mesoporous silica.

Type of silica	Maximum extraction capacity (mol/kg)	Equilibrium constant (mL/mg)
Non-doped	0.3016	0.0462
HPMSP-doped	0.3558	0.1372

4.4.1.4. Effect of pH on Zn(II) extraction

The sample pH is of prime importance for efficient retention of the trace elements on the sorbent. Careful optimization of this parameter is thus crucial to ensure the quantitative retention of the trace elements and in some cases selective retention. In this work, the influence of pH on the extraction of Zn(II) by HPMSP doped and non-doped mesoporous silica was investigated in the pH range of 2 to 5 adjusted by nitric acid. The Zn(II) ions was in aqueous solution or in 0.1 M $NaNO_3$ medium. The results were depicted in Figure 4.31.

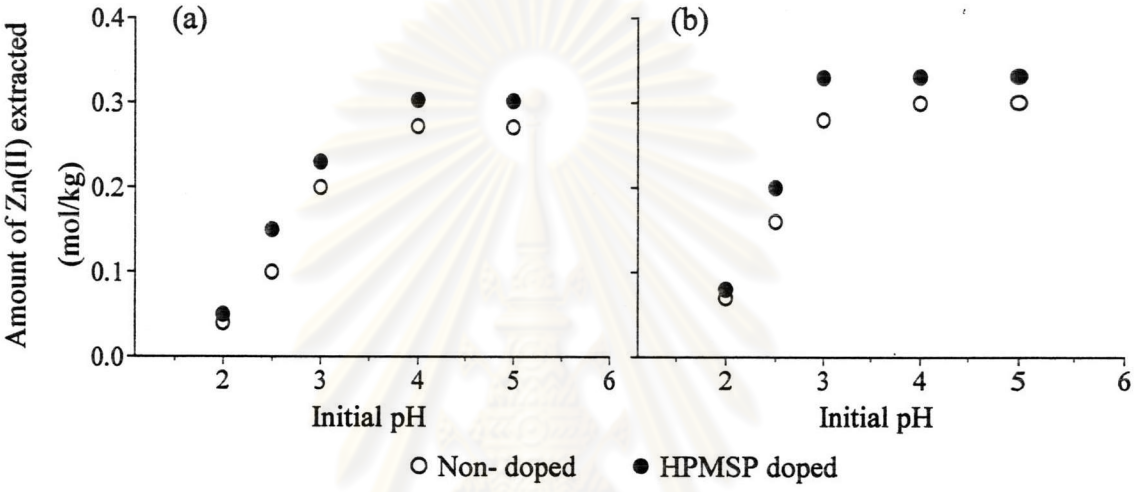

Figure 4.31 Amounts of Zn(II) extracted by non-doped and HPMSP doped mesoporous silicas from (a) aqueous solution and (b) 0.1 M $NaNO_3$ medium.

It was obviously seen from Figure 4.31 that the Zn(II) extractability of materials was poor at low pH and increased with the increasing of pH value. Indeed, as the point of zero charge (pzc) of silica was found at pH 2. So when the pH of solution was at this value the silica surface was almost silanol group (SiOH), thus the extraction was not favored. On the contrary, at pH greater than 2 the silica surface was negatively charge (SiO^-). The adsorption of Zn(II) species was thus promoted. This dissociation of silanol group on the silica surface could be expressed as:

$$SiOH_2^+ \rightleftharpoons SiOH \rightleftharpoons SiO^- \qquad (4.1)$$

Considering the effect of medium, it was found that the maximum Zn(II) extractability of both sorbents was reached at lower pH value when the metal solution contained $NaNO_3$. This phenomenon is the advantage for the application of this modified silica to the extraction of metal from industrial samples containing salts.

In addition, the amounts of Zn(II) extracted by both materials were minor different. These observations indicated that the HPMSP molecules incorporated in silica might not affect significantly the Zn(II) extraction.

4.4.1.5. Effect of foreign ions present in metal solution

The knowledge of effect of foreign ions present in metal solution is necessary prior to apply the sorbent to the extraction of metal from various aqueous samples, including natural water, seawater and industrial wastewater, which contain several salts. The influence of foreign ions on the Zn(II) extraction efficiency of non-doped and HPMSP doped mesoporous silica was thus carried out using the Zn(II) ions in aqueous solution or in 10^{-2} M HNO_3 as medium. Three salts including sodium acetate, sodium nitrate and sodium chloride with 0.1 M concentration of each were investigated. The results were displayed below.

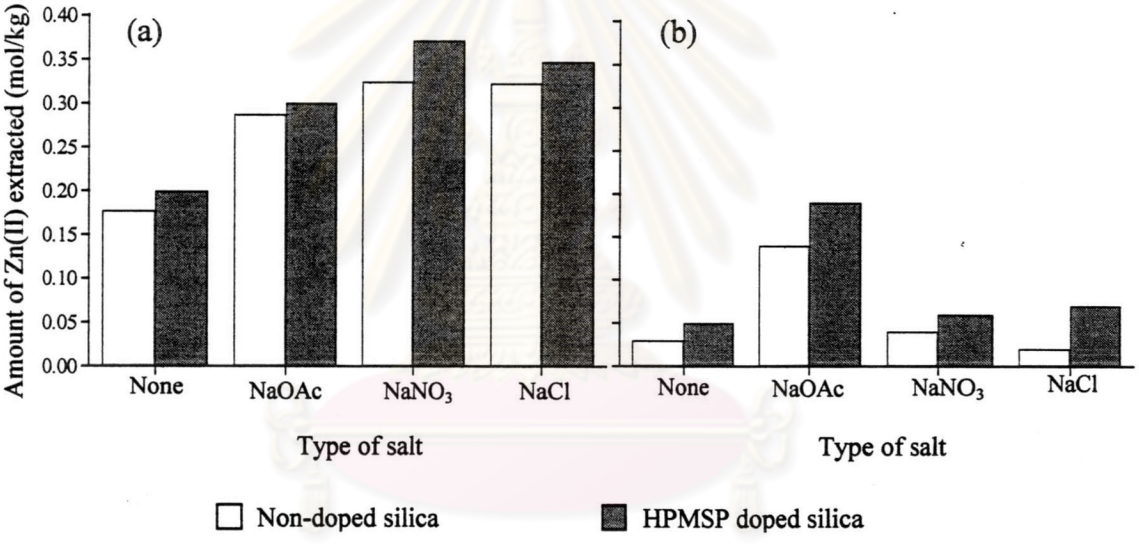

Figure 4.32 Effect of foreign ions present in metal solution on the Zn(II) extractability of non-doped and HPMSP doped mesoporous silica when the experiments were performed (a) in aqueous solution and (b) at pH 2.

It is noteworthy from Figure 4.32 that the Zn(II) extractability of both sorbents was increased with the presence of salts in metal solution. These results were probably due to the replacement of CTA^+ on the surface of silica by Na^+ present in solution. Consequently, the steric hindrance on the surface was decreased and the extraction efficiency was promoted. Furthermore, when the extraction was occurred in aqueous solution, the highest extraction was obtained when the metal solution contained $NaNO_3$ salt. On the contrary, when the extraction experiments was performed at pH 2, the NaOAc salt seemed to be the most influence salt for the

enhancement of Zn(II) extractability. This phenomenon may be caused by higher pH of the metal solution due to the hydrolysis of acetate ions. The increase in Zn(II) extraction efficiency of these materials due to the presence of salts in metal solution is the advantage when applied these sorbents to the metal extraction from real samples containing several foreign ions.

Considering the amounts of Zn(II) extracted from aqueous solution and those at pH 2 , it was found that the amounts of Zn(II) uptake were lower when the extraction was performed at pH 2. This decrease in Zn(II) extractability was probably due to the competition between the Zn(II) ions and large amounts of proton present in metal solution. Consequently, the available active site was reduced. In addition, the amounts of Zn(II) extracted by HPMSP doped mesoporous silica were higher than those of non-doped mesoporous silica for all mediums studied. These results might be due to the presence of HPMSP molecules inside the silica as previously stated.

4.4.1.6. Effect of zinc source

The influence of zinc source on the Zn(II) extraction properties of both materials was studied using different zinc salts including $Zn(NO_3)_2$, $Zn(OAc)_2$ and $ZnSO_4$. The extraction experiments were performed in aqueous solution and at pH 3 with the absence and presence of 0.1 m $NaNO_3$ in metal solution. The results were depicted in Figure 4.33.

As could be seen from Figure 4.33 (a), when the extraction was performed in aqueous solution, the highest Zn(II) extractability of both sorbents was obtained when $Zn(NO_3)_2$ was used as zinc source. On the contrary, the lowest Zn(II) uptake was obtained when $Zn(OAc)_2$ was used. These results could be explained by the steric hindrance of the acetate anion present in metal solution. The comparison between the capacities of both sorbents to the extraction of Zn(II) from aqueous solution and those at pH 3 had shown the diminution of the sorbent capacities when the extraction was performed at lower pH. This phenomenon was probably due to the effect of protons present in metal solution as described previously.

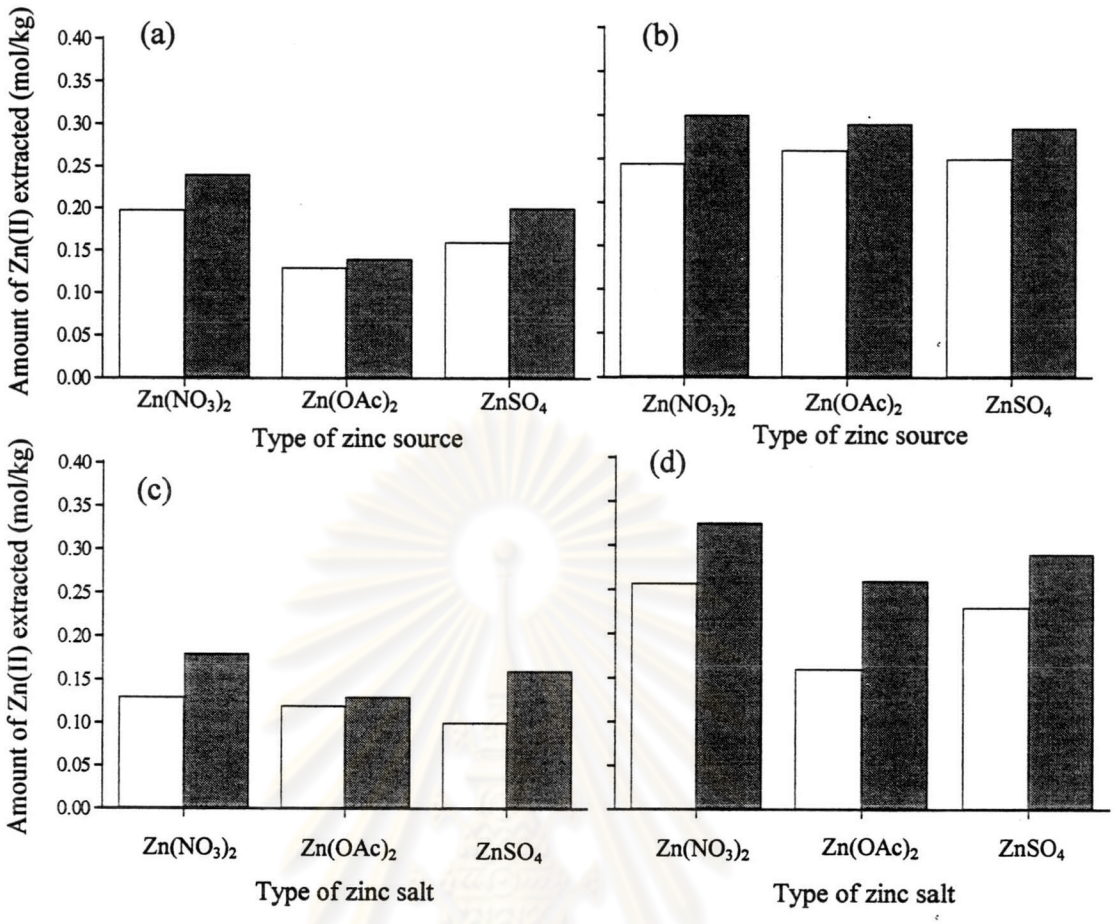

Figure 4.33 Effect of zinc source on the Zn(II) extractability of non-doped and HPMSP doped mesoporous silica from different mediums: (a) in aqueous solution, (b) in aqueous solution with the presence of 0.1 M $NaNO_3$, (c) at pH 3 and (d) at pH 3 with the presence of 0.1 M $NaNO_3$.

Considering the effect of $NaNO_3$ present in metal solution, the Zn(II) extractabilities of both sorbents were significantly enhanced with the presence of this $NaNO_3$ salt. These results seemed to be the advantage of both materials for the extraction of Zn(II) from real samples containing this kind of salt. Interestingly, for all conditions studied, the HPMSP doped mesoporous silica had higher Zn(II) extraction capacity than the non-doped mesoporous silica. This higher capacity was resulted from the anchored organic molecules as previously mentioned.

4.4.1.7. Effect of $NaNO_3$ present in metal solution

As previously mentioned in section 4.4.1.5, the presence of $NaNO_3$ in metal solution enhanced significantly the Zn(II) extractabilities of HPMSP doped mesoporous silica. In this study, the effect of this salt on the extractability of other metal ions by HPMSP modified silica was then performed. The six target metal ions

were Co(II), Cu(II), Fe(III), Ni(II), Mn(II) and Zn(II). The obtained results from triplicate experiments were displayed in Figure 4.34.

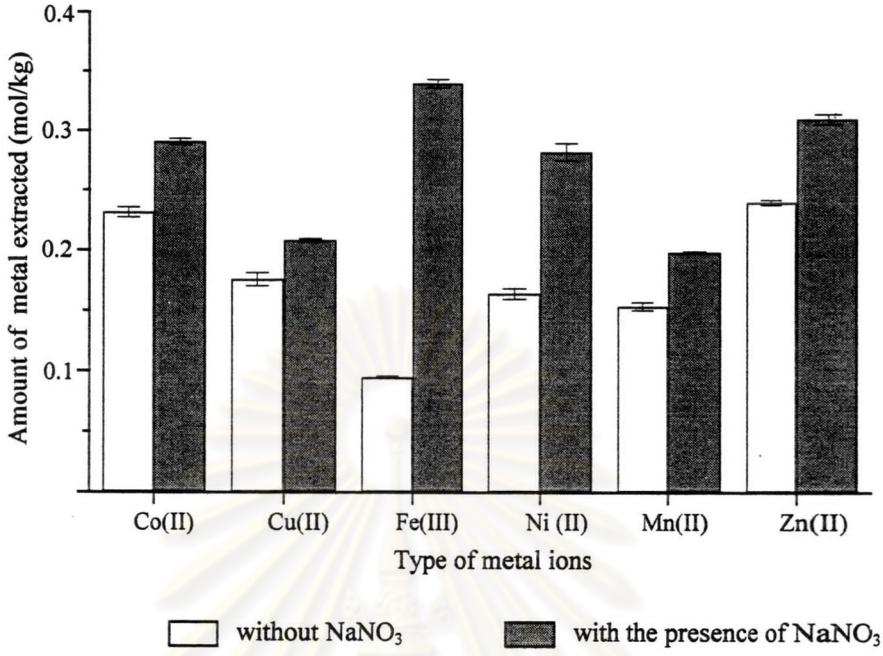

Figure 4.34 Effect of $NaNO_3$ on the extraction of different metal ions by HPMSP doped mesoporous silica.

It is obviously seen from Figure 4.34 that the presence of $NaNO_3$ in metal solution enhanced significantly the metal extractability of the HPMSP modified sorbent especially for the extraction of Fe(III). These results may be caused by the replacement of CTA^+ on the surface of silica by Na^+ present in solution. Consequently, the steric hindrance on the surface was decreased and the extraction efficiency was promoted.

4.4.1.8. Kinetic of metal extraction

The sorption kinetic studies were carried out to determine the equilibrium time of extraction of the HPMSP modified sorbent. The Fe(III), Mn(II) and Zn(II) were the three metal ions studied. The metal concentration was 200 ppm and the extraction medium was 0.1 M $NaNO_3$. The kinetic of each metal extraction experiment was performed in triplicate. The profiles of amounts of each extracted metal as a function of time for the three metal ions were displayed in Figure 4.35.

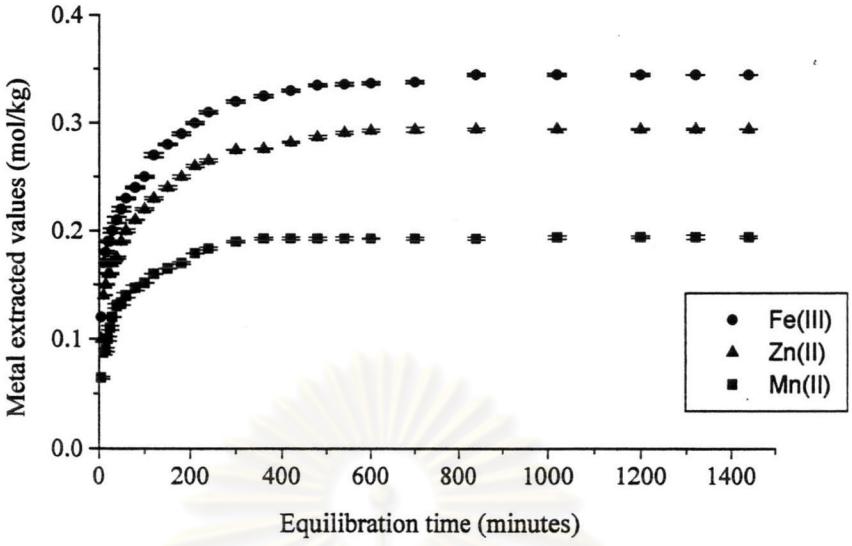

Figure 4.35 Kinetic of extraction of different metal ions by the HPMSP modified sorbent.

From Figure 4.35, the kinetic curve for Fe(III) ions revealed that the extraction of these ions was extremely rapid in the first few minutes, reached the equilibrium after approximately 480 min, and remained constant for 24 hrs which represented the saturation of the active sites of the modified material and the possible monolayer coverage of these metal ions on the sorbent surface. For the extraction of Zn(II) and Mn(II), the kinetic behaviors were similar to that of Fe(III), the extraction reached eventually a plateau within 600 min, and remained saturated until the end of the experiment (24 hrs).These results implied that the extraction time used for all previous batch experiments was sufficient to attain the extraction equilibrium. In addition, it was noteworthy that the time of 50 % sorption ($t_{1/2}$) for all three metal ions was less than 20 min. This short time indicated the rapid kinetic extraction of HPMSP doped mesoporous material.

4.4.1.9. Selectivity of material to metal extraction

The ability of sorbent to selective extraction of metal of interest from samples contained several metal ions is a prime importance. In this work, the selectivity of non-doped and HPMSP doped mesoporous silica to the extraction of metal from mixture solution of three metal ions including Fe(III), Mn(II) and Zn(II) with 66.67 ppm as a concentration of each were determined. The obtained results were displayed in Table 4.23.

Table 4.23 The amounts of each metal ion extracted by batch method from mixture solution using non-doped or HPMSP doped mesoporous silica as a sorbent.

Type of metal	Extraction (mol/kg)	
	Non-doped silica	HPMSP doped silica
Fe(III)	0.0000 ± 0.0000	0.1485 ± 0.0025
Mn(II)	0.0109 ± 0.0032	0.0390 ± 0.0025
Zn(II)	0.0828 ± 0.0032	0.1126 ± 0.0025

The results from Table 4.23 revealed that the metal extractability of HPMSP doped mesoporous silica was higher than that of non-doped mesoporous silica for all metal ions studied. It is also noteworthy for the extraction of Fe(III) that these metal ions could not be extracted by the non-doped mesoporous silica. These results suggested that the HPMSP doped mesoporous silica had strong selectivity to Fe(III) extraction. The metal extraction efficiency of HPMSP doped mesoporous silica towards the metal ions was found to be in this order: Fe(III) > Zn(II) >> Mn(II).

4.4.2. SPE column method

4.4.2.1. Determination of column capacity for the extraction of Fe(III).

Apart from Cu(II), the column capacity of HPMSP doped mesoporous silica was also determined for the extraction of Fe(III). This element became the ions of interest since it could not be extracted by the non-doped silica. So the amounts of Fe(III) extracted by HPMSP modified silica were greatly influenced only by the chelating molecules inside the sorbent. In this work, the Fe(III) extraction capacity of the HPMSP modified silica in the column was determined using Fe(III) solution in 0.1 M $NaNO_3$ medium. The range of Fe(III) concentration was varied from 100 ppm to 300 ppm. The flow rate was fixed at 2 mL/min for the whole experiments. Each concentration was performed in triplicate. The results which illustrated in Figure 4.36 revealed that the available active sites of silica on the Fe(III) extraction were saturated when the concentration of Fe(III) was greater than or equal to 200 ppm.

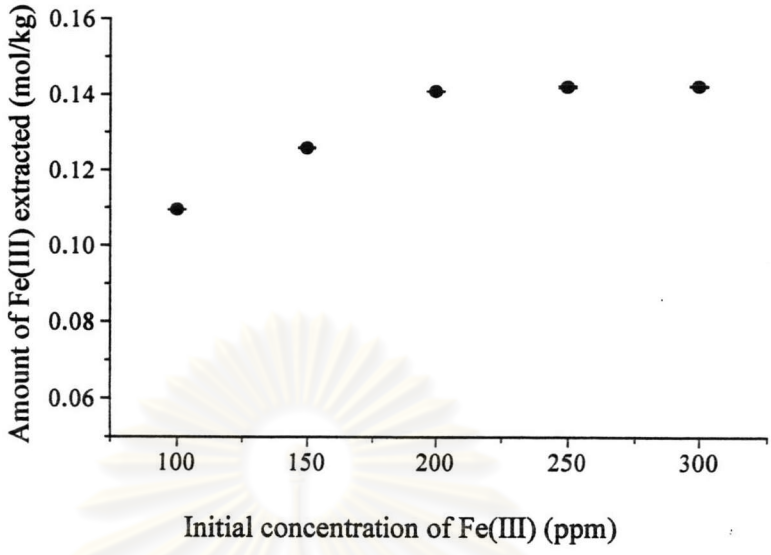

Figure 4.36 Effect of initial concentration on the Fe(III) extraction capacity of HPMSP doped mesoporous silica.

Figure 4.37 demonstrated the Langmuir adsorption isotherm type of the extraction results. The calculation from the linearization of the Langmuir plot gave the maximum extraction capacity and the equilibrium constant equal to 10.19 mg/g (0.1825 mol/kg) and 0.0167 mL/mg, respectively. This obtained extraction capacity was superior to the Fe(III) extraction capacity of other functionalized silica reported elsewhere (i.e. 0.0025 mol/kg for the Fe(III) sorption capacity of iminodiacetic groups modified silica [45], 0.0038 mol/kg for wakogel C-100 (silica gel) [46].

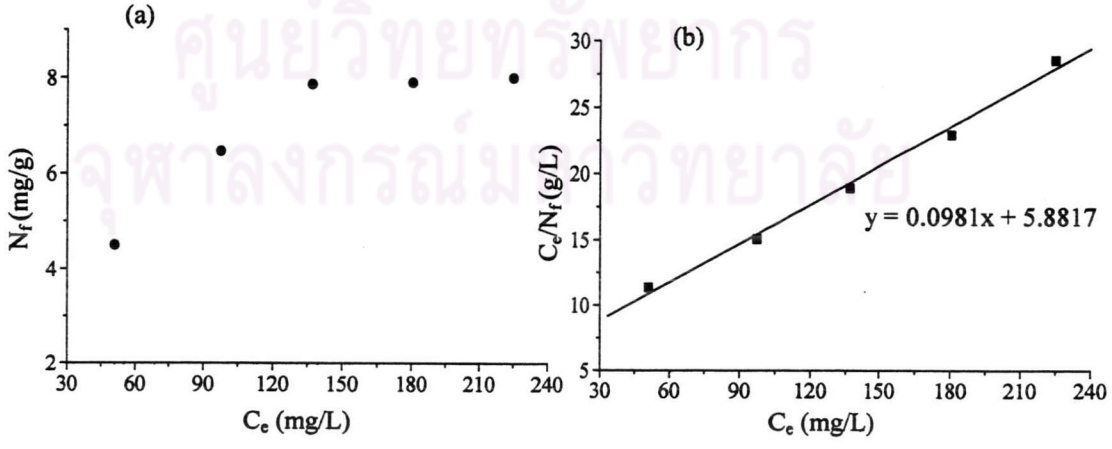

Figure 4.37 (a) Adsorption isotherm of Fe(III) on HPMSP doped mesoporous silica obtained from column experiments and (b) Linearization of the adsorption isotherm.

4.4.2.2. Selectivity of material to metal extraction.

The selectivity of sorbents to the extraction of various metal ions was also determined by SPE column method using 2 mL/min as a flow rate. The mixture of three metal ions including Fe(III), Mn(II) and Zn(II) with 66.67 ppm as a concentration of each was used. The results of metal extracted values expressed in mol/kg from three replicate experiments were exhibited in Table 4.24.

Table 4.24 The amounts of each metal ion extracted by SPE column method from mixture solution using non-doped or HPMSP doped mesoporous silica as a sorbent.

Type of metal	Extraction (mol/kg)	
	Non-doped silica	HPMSP doped silica
Fe(III)	0.0000 ± 0.0000	0.1139 ± 0.0025
Mn(II)	0.0067 ± 0.0032	0.0175 ± 0.0025
Zn(II)	0.0081 ± 0.0032	0.0252 ± 0.0025

From Table 4.24, the metal extractability of non-doped mesoporous silica was almost absent. On the contrary, the metal adsorption capacity of HPMSP modified sorbent was found to follow the order: Fe(III) >> Zn(II) > Mn(II). This order was consistent with that reported in batch method.

4.5. Application of HPMSP doped mesoporous silica to the removal of metals from industrial wastewater.

As previously mentioned, the HPMSP doped mesoporous silica can act as an effective sorbent for metal extraction. In this section, the feasibility of using this modified silica to the removal of metals from industrial wastewater sample was demonstrated.

4.5.1. Removal of Pb(II) and Zn(II)

Two sources of industrial wastewater were used in this section. The sample containing Pb(II) was collected from an electroplating factory at Bangkhen in Bangkok and the other sample containing Zn(II) was collected from a rubber factory in Chonburi. Prior to analysis, both samples were filtered through a 0.45 μm cellulose membrane. The extraction experiment was performed in triplicate using both batch and SPE column method. The sample volume used in each experiment was 25 mL. The obtained results in Table 4.25 demonstrated the successful application of this sorbent to the removal of Pb(II) and Zn(II) from industrial wastewater samples.

Table 4.25 The amounts of removed metal ions from industrial wastewater using batch and SPE column method.

Type of metal	Extraction (mol/kg)	
	Batch method	SPE column method
Pb(II)	0.0941 ± 0.0001	0.0165 ± 0.0009
Zn(II)	0.1904 ± 0.0009	0.0270 ± 0.0010

4.5.2. Removal of metals from wastewater sample containing different metal ions

In general, wastewater samples contained various metal ions. In this work, the application of HPMSP modified silica was focused on the removal of three metal ions including Fe(III), Mn(II) and Zn(II). The wastewater sample was from Bangpoo Estate in Samutprakarn. Prior to extraction experiments, the samples were filtered through a 0.45 μm cellulose membrane to remove the contaminants and capture all particles. The amounts of such metal ions containing in the samples were also determined using AAS. It was found that the content of these metal ions were below the detection limit of this instrument. Thus, to demonstrated the feasibility of using this sorbent for the removal of metals from wastewater sample containing different metal ions, it is necessary to spiked some amounts of metal ions into the sample. In this work, 34 mL of 200 ppm of each ions were spiked into 100 ml of wastewater sample. So, the concentration of each metal in the solution was 66.67 ppm. The extraction experiment was performed in triplicate using both batch and SPE column method. The sample volume used in each experiment was 25 mL. The results of each extracted ion expressed in mol/kg were compiled in Table 4.26. As seen, this sorbent could extracted efficiently all metal ions studied especially the Fe(III) ions from the wastewater sample.

Table 4.26 The amounts of each extracted metal ions from wastewater sample containing different metal ions by batch and SPE column method.

Type of metal	Extraction (mol/kg)	
	Batch method	SPE column method
Fe(III)	0.1486 ± 0.0022	0.1142 ± 0.0023
Mn(II)	0.0394 ± 0.0025	0.0176 ± 0.0025
Zn(II)	0.1123 ± 0.0023	0.0256 ± 0.0022